NASA CR-134740

DEVELOPMENT OF PROCESSING PROCEDURES FOR ADVANCED SILICON SOLAR CELLS

by J.A. Scott-Monck, P.M. Stella, J.E. Avery

HELIOTEK Division of TEXTRON Inc.
12500 Gladstone Avenue
Sylmar, California 91342

prepared for

NATIONAL AERONAUTICS AND SPACE ADMINISTRATION

NASA Lewis Reseach Center
Contract NAS 3-17350

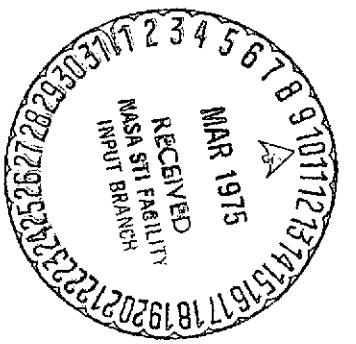

1. Report No.	2. Government Accession No.	3. Recipient's Catalog No.
NASA CR 134740		

4. Title and Subtitle	5. Report Date
Development of Processing Procedures for Advanced Silicon Solar Cells	January 1975
	6. Performing Organization Code
7. Author(s)	8. Performing Organization Report No.
J. A. Scott-Monck, P. M. Stella and J. E. Avery	
9. Performing Organization Name and Address	10. Work Unit No.
Heliotek, Division of Textron Inc. 12500 Gladstone Ave. Sylmar, California 91342	11. Contract or Grant No. NAS 3-17350
12. Sponsoring Agency Name and Address	13. Type of Report and Period Covered
National Aeronautics and Space Administration Washington, DC 20546	Contractor Report
	14. Sponsoring Agency Code

15. Supplementary Notes

Project Manager, Joseph Mandelkorn
Energy Conversion and Environmental Division
NASA Lewis Reserach Center, Cleveland, Ohio

16. Abstract

Ten ohm-cm Silicon Solar Cells, 0.2 mm thick, were produced with AMO efficiencies up to thirteen percent using a combination of recent technical advances. The cells were fabricated in conventional and wraparound contact configurations.

Processes for forming shallow junctions were successfully coupled with back surface field technology to yield both improved short and long wavelength response. Both boron diffusion and aluminum "alloying" techniques were evaluated for forming back surface field cells. The latter method is less complicated and is quite compatible with wraparound cell processing.

17. Key Words (Suggested by Author(s))	18. Distribution Statement
Silicon solar cell High efficiency solar cell Shallow junction Back surface field Wraparound contact	Unclassified-unlimited

19. Security Classif. (of this report)	20. Security Classif. (of this page)	21. No. of Pages	22. Price*
Unclassified	Unclassified	61	

*For sale by the National Technical Information Service, Springfield, Virginia 22151

TABLE OF CONTENTS

List of Figures

List of Tables

I. SUMMARY

A number of recent innovations in cell technology were evaluated and those which were mutually compatible were combined to produce 2 x 2 cm nominal 0.20 mm thick 10 ohm-cm silicon cells with AMO conversion efficiences as high as thirteen percent.

Improvement in cell collection efficiency from both the short and long wavelength region of the solar spectrum was obtained by coupling a shallow junction and a more optically transparent antireflection coating (Ta_2O_5) with back surface field (BSF) technology. In addition, improvements were achieved in the open circuit voltage and fill factor from the back surface field and a refined grid structure.

Attempts to incorporate a new contact material (Ag-Al) yielded marginal results, thus forcing us to employ the passivated silver-titanium contact system used for space flight cells. Some 0.20 mm wraparound cells using the new technology were produced and they had AMO efficiency values as high as 11.7 percent, although the typical fill factor was comparatively low due to loss of back contact area and the relatively high (10 ohm-cm) base material used on this program.

A pilot run of high efficiency BSF cells, both conventional and wraparound, were produced; and they successfully passed a variety of typical space qualification environmental tests.

II. INTRODUCTION

In the past two years, a number of new innovations in silicon solar cell technology have been demonstrated.[1,2] However, since the work in most cases had been performed by personnel more oriented towards the fundamental aspects of photovoltaic research and development, it was not known if these innovations could be adapted to the more pragmatic environment of cell manufacturing.

The purpose of this contract was to evaluate selected aspects of the new technology and to combine those found to be useful and compatible in order to produce a high efficiency cell that could be manufactured by basically conventional processes. The original goal of this effort was to produce a 0.15 mm thick, 2 cm x 2 cm, n on p cell of 10 ohm-cm base resistivity which would have an AMO conversion efficiency of 13.5 percent. Equally important, this cell would be capable of meeting the standard tests for space qualification.

Basically three innovations were evaluated: a more shallow junction which would enhance the short wavelength response of the cell, the use of a back field to increase the open circuit voltage and improve the long wavelength response of the cell, especially important for thin (0.10 - 0.20 mm) cells, and wraparound contact cell configurations which would dramatically reduce both cost and complexity in fabricating panels.

A shallow junction automatically required other changes to be made in cell processing. Since a thinner junction caused higher sheet resistance, it was necessary to develop a more refined contact configuration to compensate for the increased unit path resistance. The shallow junction increased the short wavelength response significantly, thus making the conventional silicon monoxide antireflection coating obsolete because of its high absorption of light in the region of the spectrum below 6000°A. Therefore, it was necessary to develop an alternate antireflection coating (Ta_2O_5) which was more transparent in the short wavelength region of the cell's response curve.

In addition, the shallow junction forced a reconsideration of the conventional silver-titanium contact system because it was feared that the necessary post contacting heat treatments that are done in conventional cell processing would cause degradation of the thinner junction due to impurities migrating from the titanium.

Once the basic processes for fabricating improved efficiency solar cells were derived, a run of 250 cells was made under controlled conditions. A sampling of these cells was subjected to the typical environmental tests that conventional space flight cells must pass. The results indicate that it is possible to manufacture a space qualified high efficiency cell under typical production conditions.

III. ADVANCED CELL ELEMENTS

A. Shallow Junction

The shallow junction study was judged to be one of the critical areas for investigation and consequently was the first examined in this program. The goals of this study included 1) obtaining short circuit currents (AMO) before AR coating at least 2.5 mA/cm^2 greater than those of conventional diffused cells, and 2) compatibility with all other aspects of cell fabrication developed in this program.

All diffusions were made using the conventional production methods. The source of phosphorous is phosphine (PH_3) gas which is carried in a mixture of nitrogen and oxygen. Once this mixture enters the heat zone of the furnace, a reaction takes place between the phosphine and oxygen which yields phosphorous pentoxide (P_2O_5). This compound reacts with the silicon wafer to form a phosphorous doped source glass. This method of diffusion effectively eliminates the problems that were caused when phosphorous pentoxide was used as the original source. Normally P_2O_5 reacts very easily with water vapor to form contaminating byproducts which cause nonreproducible diffusions. By creating the P_2O_5 in the heated zone of the furnace these problems are eliminated while the well understood P_2O_5 mechanism for doping is retained.

Diffusion temperatures from 800 to 900°C coupled with diffusion times from 10 to 40 minutes yielded a matrix of sheet resistances shown in Table 1. Sheet resistances ranged from 25 to 300 ohms/□. All diffusions were conducted with groups of ten 0.30 mm thick 10 ohm cm 2 x 2 cm wafers, which were then fabricated into cells for electrical performance evaluation, consisting of short circuit current and spectral response. A normal grid configuration consisting of twelve 0.1 mm wide Ag-Ti grids was used for all cells. This was felt to offer a reasonable compromise for the wide variation of sheet resistances that were obtained. Only back contacts were sintered in order to avoid degradation of the very shall front junctions which would degrade the curve shape enough to affect the true spectral response and short circuit current data. The results obtained from the electrical tests are shown in Table 2. Short circuit current values (I_{sc}) are based on measurements using a Spectrolab Model X-25 Spectrosun® solar simulator. The spectral response measurements were obtained with an equal energy calibrated filter wheel. The spectral data presented in Table 2 is in terms of a blue ratio (BR), which is the ratio of the measurement at .45 μM to that at .85 μM, the peak response, and also as a relative response value at .45 μM. The blue ratio relates the short wavelength response to material lifetime and thickness whereas the latter number relates the short wavelength response to quantum efficiency and active area. Both numbers are used in examining the shallow diffusion characteristics to exclude any anomolous results due to, for example, oversize or undersize grid lines, or wafer chips. For example, if two cells were fabricated identically, differing however in active area, (due to chips or wide grid lines) the response at .45 μM would differ in proportion to the area difference. However, the BR would be the same for both cells. Similarly an unusually thick or thin cell would produce a change in BR and short circuit current without affecting the .45 μM response.

Table 1

Diffused Region Sheet Resistance (ohms/□) versus
Diffusion Temperature and Time

Temperature	Time (min.) 10	Time (min.) 20	Time (min.) 40
900°C	38.0	25	--
850°C	84	55	39
825°C	134	88	58
800°C	312	177	111

Table 2

Cell Characteristics versus Diffusion Temperature

Temperature (°C)	Sched. (min.) Warmup-Deposition-Drive in	ρs (ohms/square)	I_{sc} (mA)	Blue Ratio (.45 μM)	Relative Response at .45μM
900	5-5-5	38.0	102.1	.48	335
900	5-15-5	24.5	97	.42	280
850	5-5-5	84.0	108	.57	405
850	5-15-5	55.4	105	.51	375
850	5-35-5	39	101.8	.46	325
825	5-5-5	134	108	.59	418
825	5-15-5	87	108.4	.56	400
825	5-35-5	58	107	.52	375
800	5-5-5	312	107.9	.58	410
800	5-15-5	177	108.1	.59	420
800	5-35-5	111	107.4	.555	405

The short wavelength response is observed to rapidly increase with sheet resistance (ρ_s) up to a value of approximately 130 ohms/□, increase slowly to a value of 200 ohms/□, and then essentially plateau at higher values of ρ_s. Figure 1 shows the cell I_{sc} as a function of ρ_s. Furthermore, no particular correlation to the diffusion temperature was observed. The junction electrical characteristics, insofar as measurement accuracy allowed, were totally dependent on the diffused region sheet resistance for the range examined, regardless of the diffusion parameters used to obtain the sheet resistance.

As a second check on characteristics of the diffused region, a sequence of diffusions was conducted at 800°C examining the impact of the ratio of deposition to drive-in times, as it was varied from 1:3 to 3:1. Inasmuch as theory might indicate a different impurity distribution in the diffused layer for the two situations, i.e, Gaussian and inverse error function, it would be informative to see if any electrical differences could be noted. Again, no particular relationship was observed beyond a slight difference in ρ_s, as expected. As shown in Table 3, cell characteristics are quite similar with the only differences being attributable to long wavelength response differences. Additionally a number of wafers with relatively deep diffusions (ρ_s= 40 ohms/□) were etched to remove various amounts of diffused region so that final ρ_s values varied from 80 to 150 ohms/□ . When fabricated into cells, they showed precise agreement with corresponding cells (i.e. same ρ_s) produced directly through normal diffusion.

Consequently, all experimental evidence pointed to a strict correlation between diffused region electrical characteristics and sheet resistance over the range of variables examined. For all practical purposes this range covers the limits of usefulness for high volume diffusion processing, i.e. higher temperatures would reduce diffusion uniformity while lower temperatures would severely limit cell production.

The results indicate that for a typical 0.30 mm thick 10 ohm cm cell, an optimum BR of .59 to .60 can be achieved for a ρ_s range of 100-175 ohms/□. Lower values of $\rho_s$will reduce short wavelength response and higher values, although showing no appreciable short wavelength response gain, result in junctions easily degraded during typical post diffusion heat treatments. With $\rho_s \leq 175$ ohms/□ it is possible to weld and solder cells without severe degradation. Furthermore, based on X-25 solar simulator measurements an I_{sc} increase of approximately 2 mA/cm^2 over conventional bare cells was observed at ρ_s = 175 ohms/□. However, the X-25 is considered to be slightly short wavelength deficient when compared to the AMO spectrum and tests with a pulsed xenon simulator show greater increases. Therefore, 2 mA/cm^2 is taken as a conservative estimate of the gain obtained from a shallow diffusion.

Although the shallow junction optimization was conducted during the earlier portion of the program, an additional filter position was calibrated at .4μM on the Heliotek filter wheel using data supplied by NASA/Lewis and although remeasurements of the earlier fabricated cells at this position

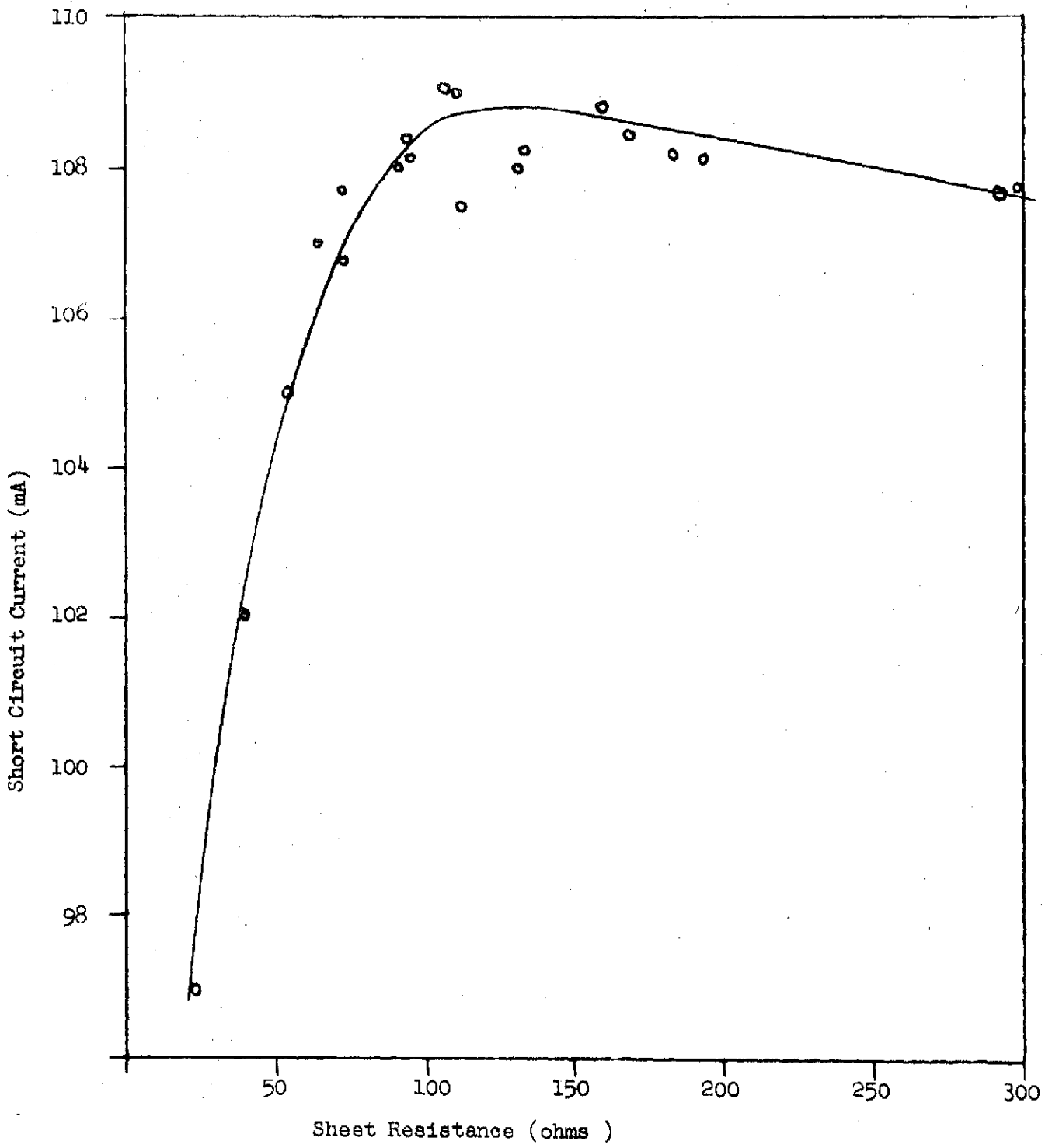

Figure 1. Short Circuit Current (bare cell) vs. Diffusion Sheet Resistance

Table 3

Impact of Deposition-Drive In Time Ratio
on Junction Electrical Output

Temperature (°C)	Sched. (min.) Deposition-Drive in	ρs (ohms/square)	Blue Ratio (.45 μM)	Relative Response at .45 μM
850	5-15	81	.55	390
850	10-10	70	.55	400
850	15-5	65	.53	390
825	5-15	110	.58	420
825	10-10	96	.56	390
825	15-5	99	.56	410
800	5-15	194	.595	425
800	10-10	175	.59	427
800	15-5	180	.59	416

substantiated the above conclusions, it was noted that the response increase at .4μM was as great as 35 percent, compared to the 20-25 percent enhancement at .45μM. A typical optimized cell response in shown in Figure 2 compared to a conventional cell. Although the magnitude of the response at .4μM might be somewhat in error, percentage increases are considered accurate. The impact of the diffusion depth can be observed even at a wavelength of .7μM-.75μM, although substantially reduced.

B. Contact System

Since very shallow junctions are susceptible to degradation from fast diffusing impurities that originate in the titanium "glue" layer of the silver-titanium system[3] work on a replacement contact system was undertaken. The basic problem that must be solved involves the titanium component of the basic space qualified contact system; and thus our efforts concentrated on substituting another metal for titanium while retaining the high conduction component, silver, of the present contact.

Although aluminum is a shallow acceptor in silicon, its thermodynamics are such that it was a potential candidate to replace titanium. Aluminum will alloy with silicon at temperatures above 577°C, but the amount of silicon taken up in this reaction is a strict function of the amount of aluminum available. Thus very small amounts of aluminum, in principle, can be alloyed into the junction without shorting the cell. This is due to the fact that the maximum solubility of aluminum acceptors in the regrowth region will be at least an order of magnitude below the concentration of phosphorous donors provided the penetration depth is less than half of the junction depth.

Aluminum if alloyed slightly into silicon would form a strong bond. Silver alloys readily with aluminum at temperatures as low as 150°C and at a temperature of 550°C will form an alloy that is roughly twenty (20) atomic percent silver,[4] thus forming a strong bond between the aluminum and the silver. Therefore, if an aluminum silver composite were deposited on silicon and subsequently heated to 575-600°C the two alloys would be formed so that an adherent bond between the silicon and the silver would be formed by means of the Si-Al and Al-Ag alloys.

Small amounts of high purity aluminum were evaporated from a tungsten coil onto cells and then a deposition of production quality silver was made from a tantalum dimple boat that was heated separately. Since we did not have a thickness monitor available, an extrapolation was made from previous data on aluminum weight and deposition thickness measured, to derive the amount of aluminum necessary to yield deposition thicknesses in the order of 500 to 1000Å. Silver thicknesses of between three and five microns were typically deposited over the aluminum.

Upon removal from the vacuum system, it was found that the silver was peeling from the cells. In some cases this peeling did not occur immediately but took place over a period of five to ten minutes after removal from vacuum. It was suggested that the delay between the aluminum and silver depositions was allowing a thin layer of contaminants to form on the aluminum thus preventing the silver from adhering. Attempts were made to decrease this and the results were better, but still not acceptable.

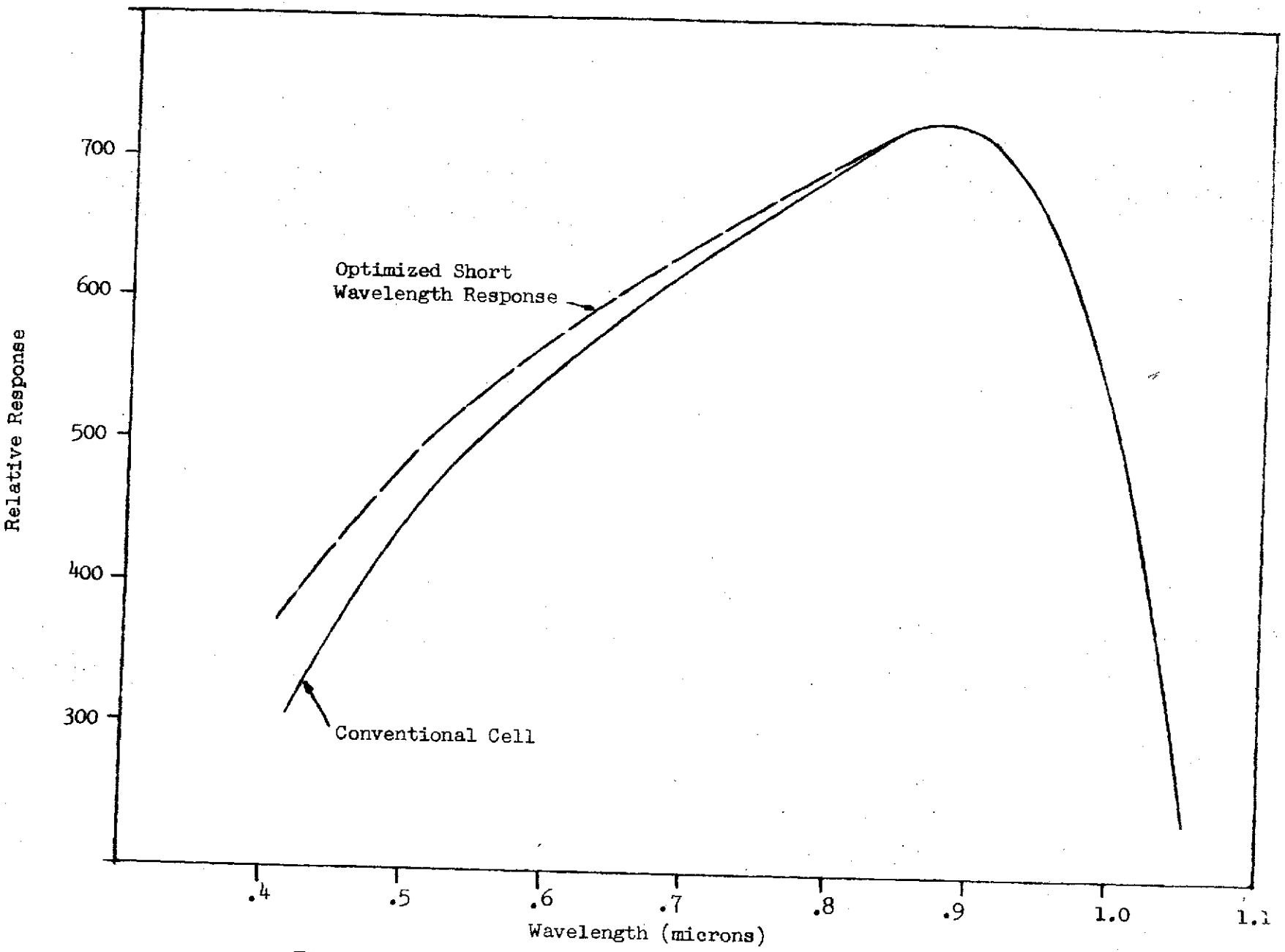

Figure 2. Shallow Junction Spectral Response

Rather than continue with this work, we decided to retain the conventional silver-titanium system, but to eliminate sintering of the front contact. Naturally this made cell fabrication slightly cumbersome due to the requirement of performing two separate depositions, but it allowed the other phases of the program to progress. Since the cells were to be solderless, palladium was used to passivate the contact against humidity induced degradation.

It should be mentioned at this point that there is some controversy concerning the function of sintering. From our experience we have concluded that sintering is only necessary for improvement of the electrical characteristics of the cell, although there have been claims that this process also improves contact adherence. All cells fabricated for this program successfully passed standard tape peel tests. In addition, some number were soldered and the contact pull strength was determined to be above typical requirements (500 gms). There was no significant difference in pull strength between the unsintered front and the sintered back contact.

C. Contact Configuration

The basic contact configuration for solar cells consists of a number of narrow gridlines (~.35 mm wide) running from the edge of the cell to a collector bar located at the opposite edge. The dimensions of the collector bar are determined by the particular interconnects that are to be used in assembling the cell into a panel; typically the collector bar is from .90 to 1.25 mm in width and runs the length of the cell. For a typical 2 x 2 cm production cell, the contact area covers approximately ten (10) percent of the active surface.

The spacing and number of gridlines is determined by many design parameters such as the sheet resistance of the diffused layer, the base resistivity of the cell, the load point required and the conductivity and thickness of the contact material itself. A number of theoretical analyses have been made of this design problem, and we adopted the work of Wolf in order to develop an optimized grid pattern.[5]

The key design parameter is the sheet resistance of the diffused layer; and as the resistance increases, the spacing between grids must decrease in order to avoid a significant increase in the series resistance of the cell. The power curve of the cell is significantly influenced by series resistance, becoming more rectangular as series resistance is reduced. However, as the spacing between gridlines is reduced, the amount of active area covered by the increasing number of gridlines tends to compromise the cell's performance.

To avoid a reduction in active area, it is necessary to reduce the width of the gridlines. However, it now becomes important that the contact metallization thickness be increased to avoid introducing additional series resistance from the contact configuration. Thus the design and implementation of a more refined contact configuration becomes a very practical problem in mask design.

For the sheet resistance range we were considering, namely 100 to 200 ohms/□, the analysis showed that fourteen (14) to eighteen (18) equally spaced lines would provide a minimum in series resistance. If the lines were to be of normal width (.15 mm), over twelve (12) percent of the cell active area would be lost. According to the analysis, it is only necessary to have lines .03 mm wide provided that the silver thickness was at least 2.5μM thick.

Conventional solar cell grid finger fabrication consists of vacuum evaporation of contact materials through metal masks onto the solar cells. The masks are formed by photo-etching thin (75μM) stainless steel foil with the desired grid pattern. Although this process involves a minimum number of steps and is readily applicable to high volume, the use of such masks for forming narrow grids is limited to a minimum width of .10 mm, considerably larger than the calculated optimum grid width. The restriction to rather large dimensions is due to the isotropic etching of the metal, which restricts minimum width to the sum of metal thickness and photomask opening size. For the thinnest practical metals this limit is 0.1 mm.

There are two possible methods of obtaining line widths less than 0.1 mm; photoresist and bimetallic masks. The former approach was not considered because the process is relatively complicated and, therefore, in violation of the contract goal which was to develop a cell that could be fabricated in quantity under typical manufacturing conditions.

Consequently, a modified form of the original metal masking technique, a bimetallic mask, was employed. The bimetallic mask consists of a sandwich of nickel (5μM thick), beryllium copper, (175μM thick) and nickel (5μM thick). One side of the sheet is selected to be the finished surface; i.e., the surface which will be against the solar cell during the contact deposition. On this side the desired grid pattern is photo-etched using dimensional tolerances of 5μM or better. As a minimum, a grid width of .025 mm can be etched. The desired grid pattern is also etched out on the side opposite the finished side, although the etched pattern is larger with more generous tolerances. In cross section, then, the etched regions appear V shaped, with the small opening on the finished surface, and the wide opening on the side opposite. Consequently, when placed in the vacuum chamber, the large openings will face the source, allowing the evaporating metal to reach the small openings on the finished side, and go through to the cell. In this manner the finished surface becomes a thin mask, with the advantage of narrow grid definition, and the remaining portion of the mask is used primarily for mechanical support.

Figure 3 shows a bimetallic mask assembly consisting of the bimetallic mask, the mask support frame, and the cell holder frame. Various configurations were designed and purchased. Masks with twelve (12), fourteen (14) and eighteen (18) gridlines were used. To conserve active area, the collector bar was reduced from a 0.1 mm to a 0.05 mm width. The majority of the cells that were fabricated for delivery used masks that had eighteen (18) equally spaced 50μM wide gridlines connected to a 0.05 mm wide collector bar. This gave a total active area of 3.73 cm^2 on the 2 x 2 cm cells used on this program.

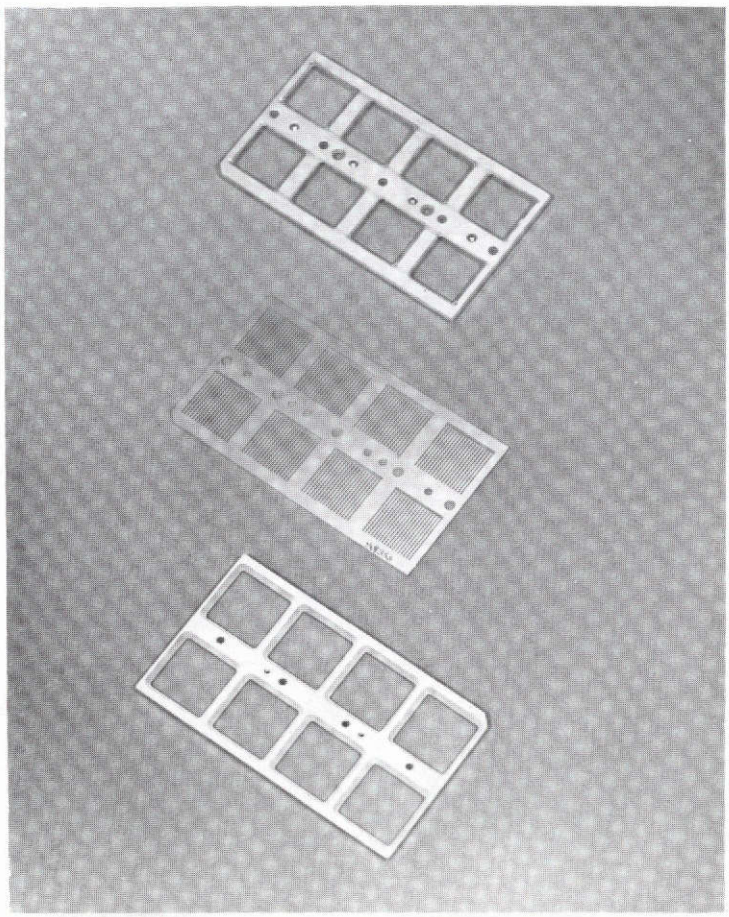

Figure 3. Bimetallic Mask Assembly (Top-cell holder frame; middle-bimetallic mask; bottom-mask support frame)

The bimetallic masks allow normal manufacturing contact evaporation processes to be used. As with most innovations, there are a number of new problems. The gridline openings tend to fill up with silver more rapidly because of their narrow width, and this requires more frequent cleaning. The nickel overcoat is more easily damaged in handling and cleaning, resulting in a shorter useful lifetime. However, these problems are not insoluble; and it can be said that this type of mask does allow shallow junction cells to be manufactured in volume using conventional processes.

D. Fabrication and Evaluation of Back Surface Field (BSF) Cells

The goal of this phase of the program was to reproducibly achieve cells with open circuit voltages (V_{oc}) of .58 V minimum using .150 mm thick 10 ohm-cm n/p cells. The BSF would be formed using boron as the dopant.

The initial boron BSF work was based on our earlier work with boron trichloride (BCl_3) for manufacturing P/N lithium doped solar cells.[6] However, diffusion times and temperatures were increased to provide greater penetration since previous work on aluminum BSF cells had indicated an increased cell output with increased field depth. Diffusion temperatures were 1050°C and 1100°C with time varied from 90 minutes to 120 minutes. The shallowest diffusion thus obtained had ρs = 9 ohms/$\square$, as measured on N-type surrogates included with the .150 mm thick P-type samples. The deepest diffusion showed a ρs = 4.5 ohms/$\square$.

The N-type samples were then angle lapped and stained; and by using optical interference techniques, the diffusion depth was found to vary from 0.9 μm for the ρs = 9 ohm/$\square$ wafers to 1.5 μm for the ρs = 4.5 ohms/$\square$ wafers. At this time these depths were felt to be sufficient for BSF work and the P-type wafers were fabricated into cells in the following manner:

Following the boron diffusion it is necessary to remove the diffused layer from one side of the wafer in order to properly form the junction by a subsequent phosphorous diffusion. The predetermined P+ side is masked and the wafer is dipped in hydrofluoric acid for 30 seconds, then immersed in 3-1-2 (HNO_3-HF-CH_3 COOH) acid, followed by a quench in deionized water. The 3-1-2 immersion time is determined by the amount of material to be removed and acid temperature, so consequently etched wafers are tested with a hot point probe in order to establish an etch time for a particular boron diffusion lot. Normally a few minutes is sufficient.

Following the etching, the masking is removed and the wafers are given a phosphorous diffusion. The boron diffusion glass residue on the P+ side is then removed and cell fabrication is completed in the normal fashion.

Initial cell performances were poor, with V_{oc} on the order of 550-560 mV, compared to 540 mV for non-BSF control cells of a similar thickness. Furthermore, severe breakage occurred with the .15 mm thick wafers during fabrication.

The combination of thin cells (down to .125 mm) and the additional boron BSF fabrication steps proved to be quite unwieldy. Consequently, the wafer size was increased slightly to .20 mm, yielding a much higher number of finished cells.

Since it was likely that lack of process control, especially in masking and etching, was the main cause of the unexpectedly low values of V_{oc}, alternate methods for processing boron BSF cells were examined.

Masking techniques using wax and tapes were compared. The waxes were found to be unsuitable not only because their use required much handling, but also because of wax leakage around the cell edge. This led to the occurence of small unetched regions on the wafer face which would remain P+ after the junction diffusion. Then, with subsequent contacting, these regions would cause severe device leakage if bridged by the N+ contact. In contrast, the tape technique produced a cleanly etched surface with some slight undercutting on the P+ rear surface. However, with subsequent edge etching these thin, undercut areas (N+ following the N+ diffusion) would be totally isolated electrically. Consequently, although still cumbersome, the tape masking method was retained.

A second major fabrication problem involved the glassy-like boron oxide/nitride layer formed during the initial diffusion. It was found necessary to have a thick durable layer which would later protect the boron diffusion region during the phosphorous diffusion. However, it was also necessary that this layer be etched off one side readily without causing non-uniform etching (staining) of the silicon in the step prior to the N+ diffusion. Finally, it was necessary that this layer be removable after the N+ diffusion to allow for contacting without affecting the N+ diffusion.

Obtaining such a boron "glass" layer required altering the boron trichloride, oxygen and nitrogen flow rates for each temperature range used. Since actual flow rates are highly dependent on the particular furnace temperature profile, tube size, diffusant time and wafer location, only the following generalizations will be made. Excessively high oxygen levels were found to produce easily etched boron layers which would not hold back the phosphorous diffusant, and excessively low oxygen flow rates led to the build-up of extremely durable boron glass layers which, although capable of masking the N+ diffusion, would not etch off uniformly, causing staining of the silicon surface.

Although parameters have been adjusted to provide a workable boron glass layer, this process still needs further work for large scale production. However, suitable gas flow rates were established to allow for fabrication of devices under this contract. Using the improved masking and etching techniques and greater cell thickness, additional boron BSF cells were fabricated about halfway through the problem. These were done at temperatures varying from 1000°C to 1100°C.

This time cells with high V_{oc} were achieved at all temperatures, with surprisingly little difference noted between low temperature shallow BSF ($<.5\mu M$) cells and deep ($>1\ \mu M$) high temperature BSF cells. Although there was little indication of shunting, cell efficiency was low due to low short circuit currents.

Spectral response measurements showed that indeed the cells were low in response from .75 to .95 μM, although oddly at 1.05 μM the response was reasonably good. Again these values are relative, and when compared to a conventional (non-BSF) 200 μM thick cell would be considered good. However, when compared to aluminum BSF cells fabricated in the past at Heliotek, the mid and long wavelength response was deficient by approximately 15 percent. Analysis of the spectral response data along with lifetime measurements conducted at NASA/Lewis both indicated lifetime degradation.

Since V_{oc} values exceeding 590 mV had been observed (a 50 mV gain over conventional 200 μm thick cells), it was plain that further BSF cell output enhancement required that the lifetime degradation be minimized or eliminated. A number of approaches were tried, including post BCl_3 diffusion cooling schedules, annealing, pre-diffusion wafer cleaning and even an alternate boron diffusion method using B_2H_6.

Wafers diffused with the latter source were provided to Heliotek by NASA/Lewis for processing beyond the boron diffusion step. However, in all cases the B_2H_6 oxide layer was found to be overcome by the phosphorous diffusion eliminating any BSF effect. Since insufficient time was available for investigating a phosphorous masking technique, the $BC\ell_3$ diffusion was used for all further work.

Based on our previous work on $BC\ell_3$ diffused P/N cells done a number of years ago, a specific cooling cycle has been used for all $BC\ell_3$ diffusions, including the BSF cells. This step consists of pulling the diffused wafers to a zone set at 700°C where they remain for one half hour. Following this the wafers are removed from the furnace and allowed to cool to ambient while still on the diffusion boat. This simple step has in the past helped maintain a uniform lot lifetime (as determined by spectral response) whereas eliminating the 700°C dwell often yielded a number of unusually low lifetime cells.

It was decided to try a 700°C anneal after the phosphorous diffusion in order to see if lifetime could be maintained after the repeated diffusions In the first test a one half hour anneal at 700°C was used with half a group of BSF cells. These were then compared with the non-annealed half and found to have approximately 5-10 percent more response in the mid and long wavelengths, an indication of improved lifetime. V_{oc} for both groups were identical at 570 mV (uncoated). However, both groups long wave response and, hence, lifetime were still lower than that observed for aluminum BSF cells.

Consequently, a second test was conducted with an increased anneal time (two hours). In this case both annealed and non-annealed groups showed similar V_{oc}'s, 587 mV (no AR), the highest obtained up to that time, in part due to improved fabrication techniques. However, I_{sc} and spectral response were both low, indicating no improvement in lifetime. Rather than continuing the annealing work which so far had been only sporadic in helping the lifetime, the NASA/Lewis contract monitor suggested that the lifetime degradation might be due to heavy metal impurities contaminating the wafer surfaces and proposed precleaning prior to the diffusions, in particular the boron diffusion.

Normally wafers are cleaned before diffusion by degreasing in trichloroethylene and alcohol, although in some cases wafers are etched in HF acid for a short time to reduce any oxide buildup. This process was altered by adding an additional step just prior to the boron diffusion. This cleaning process, referred to as the "PNH" cleaning method by the semiconductor industry, includes hydrogen peroxide, ammonia and hydrochloric acid, and is commonly used to remove heavy metal residues from silicon surfaces. Furthermore, a less involved HCl immersion was added just prior to the phosphorous diffusion step, since it was felt that the boron diffusion was more influential in introducing lifetime degrading impurities and thus required a more rigorous preclean. At this time the boron diffusion temperature used was 1000°C, with a diffusion time of 45 minutes, since higher temperatures had not yielded any better BSF performance.

Examination of the special preclean BSF cells showed an immediate gain of 1 mA/cm^2 with a 10 percent increase in long wavelength response. NASA/Lewis measurements corroborated the increase in device lifetime. A number of additional tests verified the increased long wavelength response observed in the first test; consequently, the PNH preclean was retained for all additional BSF work. At the best, boron BSF cells formed with the preclean compared quite favorably with aluminum BSF cells, a noticeable improvement from the earlier results. However, it should be mentioned that the best aluminum BSF cells were still somewhat higher in long wavelength response than the best boron BSF devices, indicating some room for improvement. Continuing lifetime measurements at NASA/Lewis have indicated that at present the diffusion length in the boron BSF cells is comparable to device thickness (200 μM). In contrast, the diffusion length obtained prior to the preclean generally ran from 100 $\longrightarrow$ 150 μM.

It is worth noting that throughout the boron BSF work, excepting the very initial devices where shunting was a problem, the V_{oc}'s have been quite high. In general, the 580 mV minimum has been achieved on the large part in all completed devices. However, the I_{sc} has varied from poor (135 mA typical) to good (150 mA typical) independent of the V_{oc}, suggesting different mechanisms for each.

In Figures 4 through 6 typical I-V curves are presented for boron BSF cells fabricated during this program. All wafers were 200 μM thick, except where noted, 10 ohm cm P type material, with a phosphorous diffusion yielding a ρs = 100-150 ohms/$\square$. A typical spectral response is shown in Figure 7.

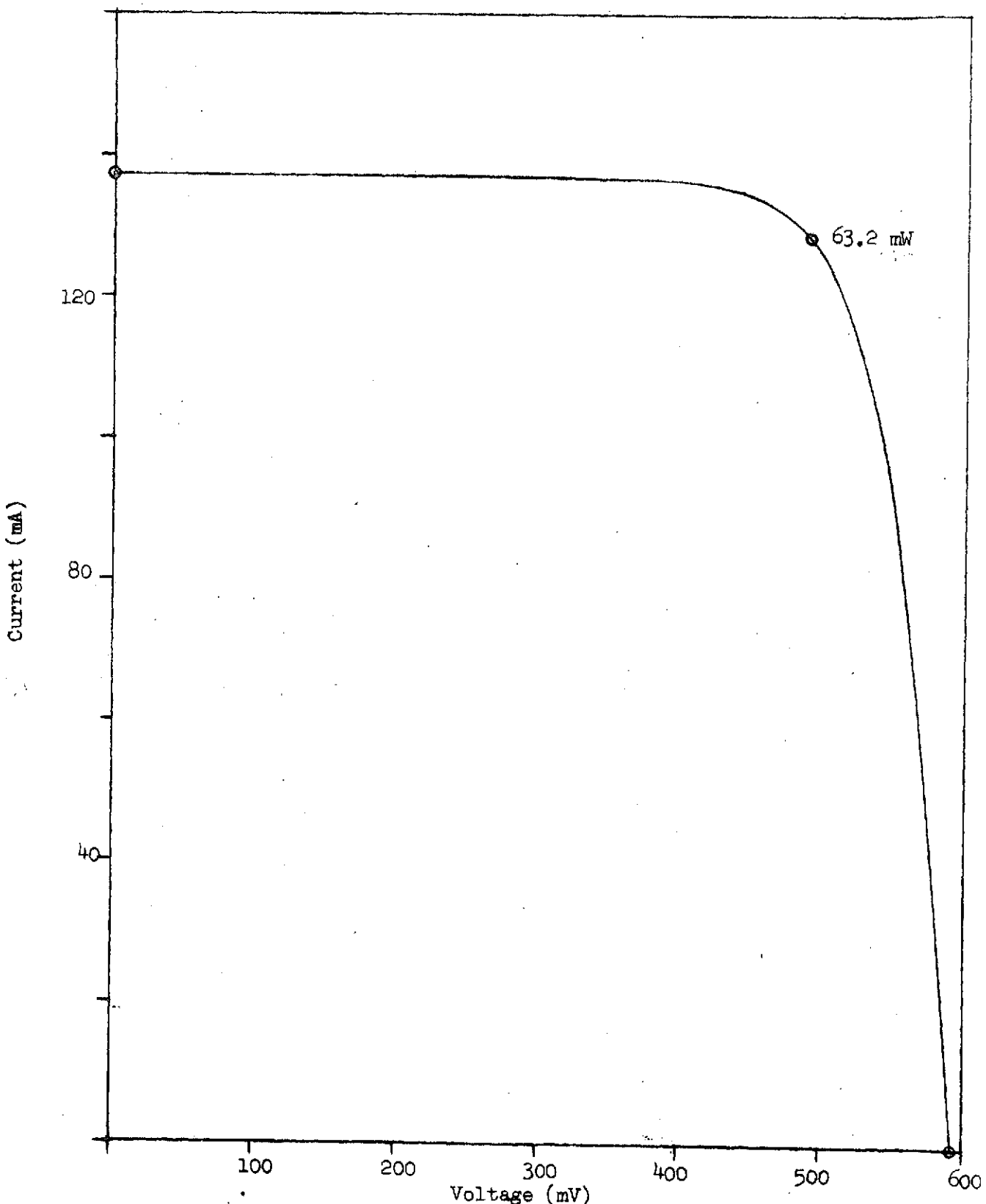

Figure 4. Typical Boron BSF Cell V-I Characteristic

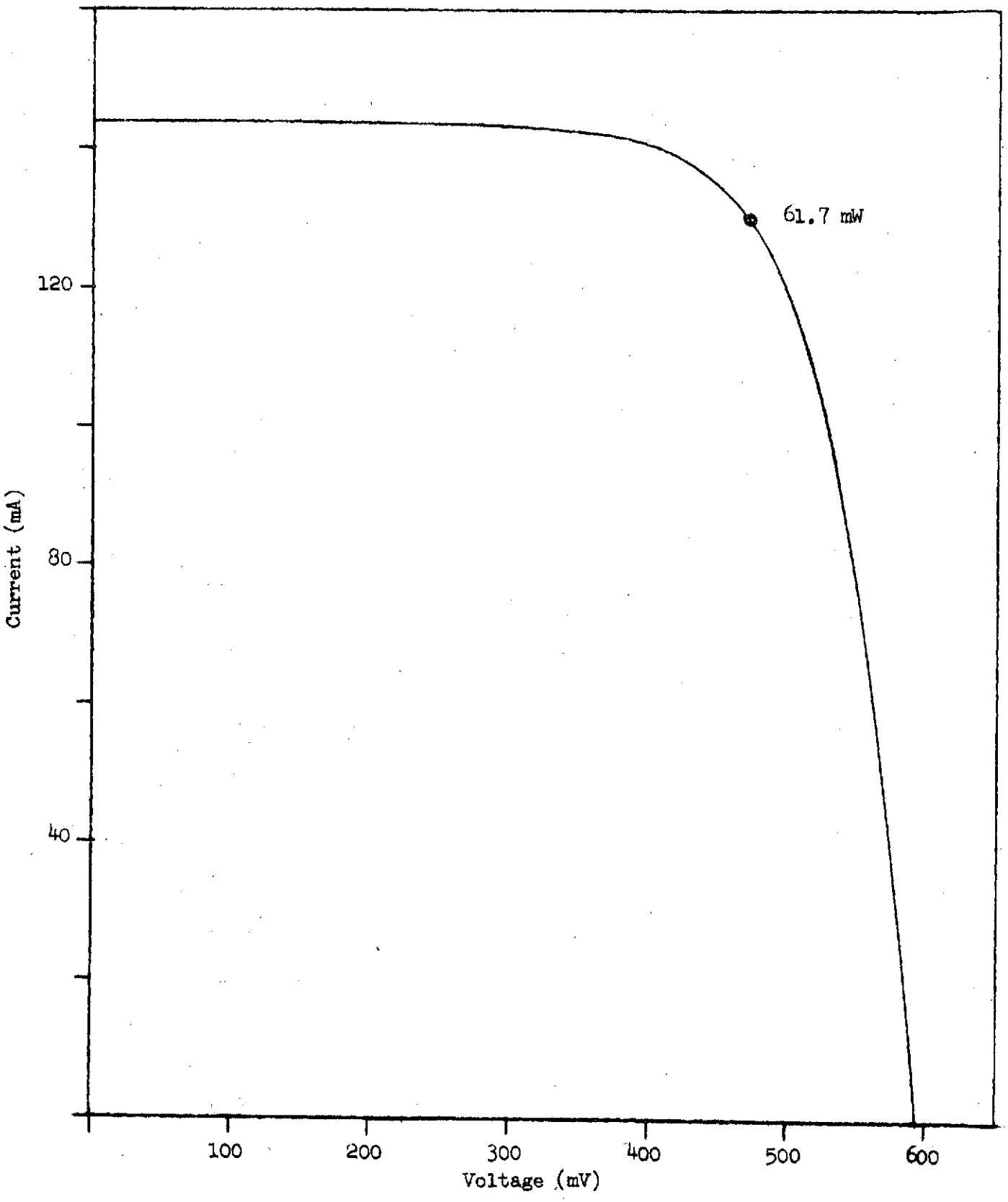

Figure 5. Typical Boron BSF Cell V-I Characteristic

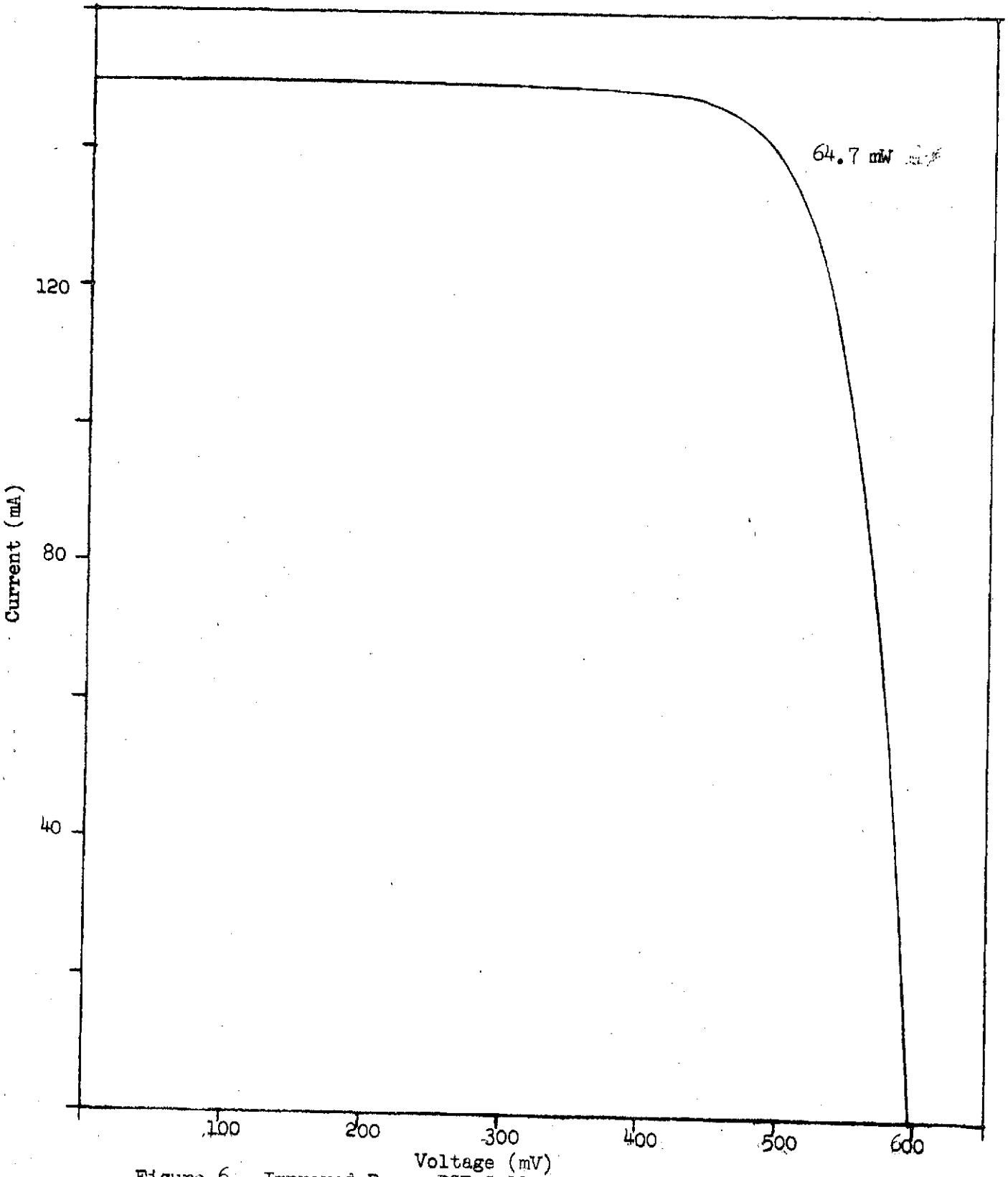

Figure 6. Improved Boron BSF Cell V-I Characteristic

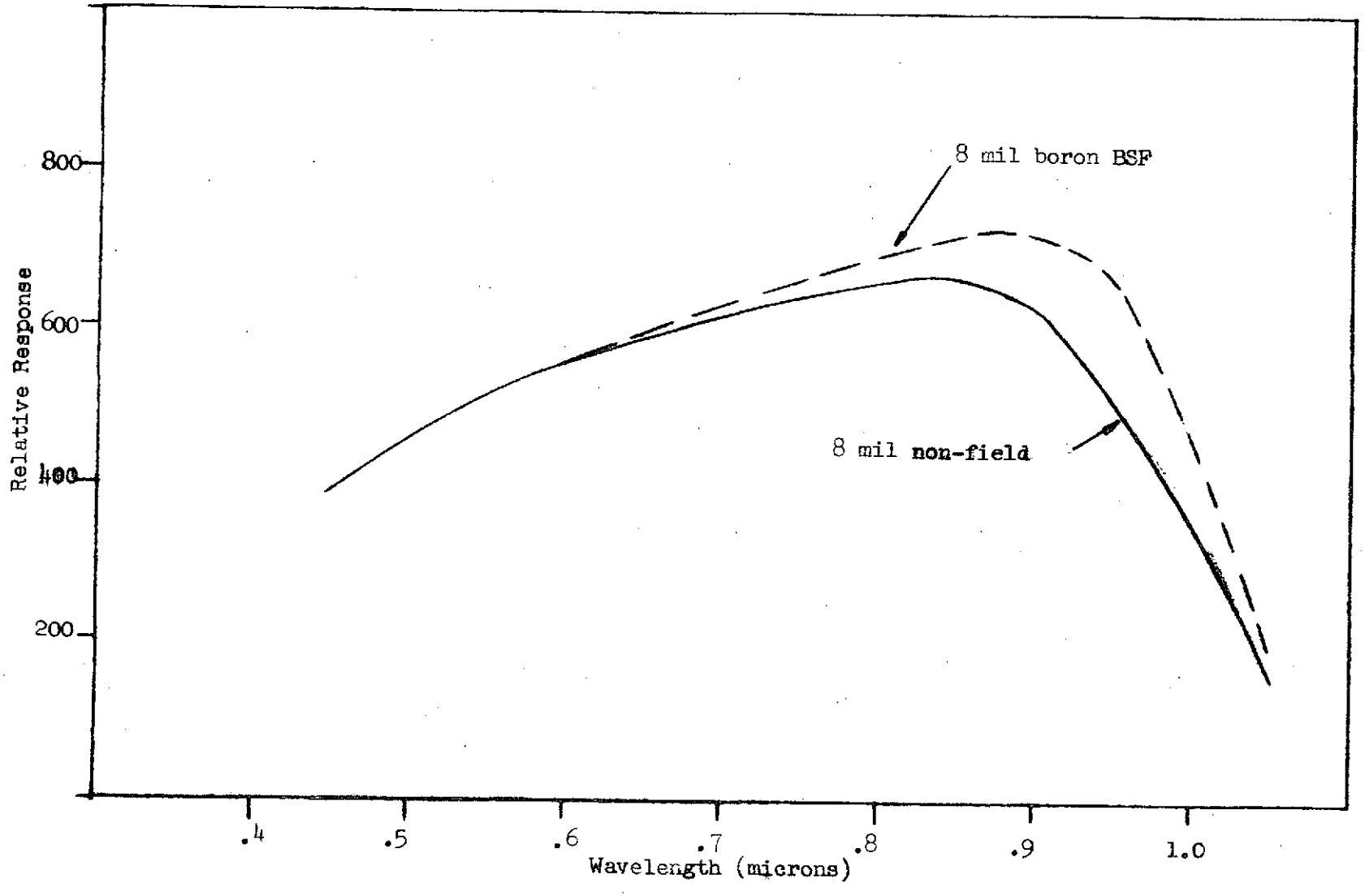

Figure 7. Improved Boron BSF Cell Spectral Response

E. Aluminum Back Surface Field

As was shown in the previous section, the use of boron as the acceptor dopant for forming a back surface field in the cell is a rather complicated process. While the necessary boron process controls were being derived, we investigated aluminum as a dopant source, using our previous experience in this area.

Results using aluminum indicated that there was little difference in cell output whether boron or aluminum was employed. The boron cells appeared to have slightly higher values of open circuit voltage, but the aluminum cells showed slightly better short circuit current outputs.

This difference in cell output can be understood by comparing the two processes. In the case of boron, a relatively high temperature diffusion ($> 1000°C$) is required to develop the field. This probably results in contamination of the wafer by fast diffusing impurities which act to reduce the minority carrier lifetime. This theory can be supported in light of the success that was achieved by using special cleaning procedures prior to the boron diffusion. In contrast the aluminum process requires significantly lower temperatures and the molten aluminum may act as a sink for unwanted impurities.

If the assumption is made that the surface concentration of acceptor dopants is influential in determining the open circuit voltage, then one would expect boron which dopes the surface to $\sim 5 \times 10^{20}/cm^3$ to yield higher voltages than aluminum, whose maximum solubility is at least an order of magnitude lower.[7)]

From a manufacturing point of view, the aluminum process is the more mature since it requires fewer operations. Aluminum is deposited by vacuum evaporation methods and then heated to temperatures from 800 to 900°C for periods from ten to forty minutes. This can be done either on a diffused wafer or simultaneously during the diffusion itself. In either case, the molten aluminum takes up a significant amount of silicon which either completely eliminates the previous diffused layer or masks against the diffusion when the process is done simultaneously.

It should be pointed out that there is a relationship between the amount of aluminum deposited and the resultant open circuit voltages. Evaporated layers at least five microns thick are required for high open circuit voltages (> 580 mV). Layers up to twenty microns have been deposited, but the open circuit voltage seems to saturate as a function of aluminum thickness above five microns. We do not completely understand this process and feel that thinner layers of aluminum should work as well since the field is formed by the diffusion of aluminum from the evaporated layer itself and not from the alloy region that develops.

Naturally the rather large amounts of aluminum presently required for optimization of cell output cause some problems. Occasionally localized areas will actually penetrate completely through the silicon blank. In other cases severe "bowing" of the cells will occur. This "bowing" is eliminated during the subsequent cleaning step after field formation, but in the case of thin cells the breakage in handling can become extreme.

The cleaning process after field deposition is important both from an electrical as well as a mechanical standpoint. The aluminum residue does not allow an adherent contact to be reliably formed and it also acts to lower the open circuit voltage because the aluminum surface layer reacts with the carrier gas to form an insulating region.

Cleaning is achieved by boiling the cells in hydrochloric acid until all evidence of reaction is eliminated. Then the cells are placed in water and given an ultrasonic cleaning which removes all traces of the aluminum residue. The silicon surface is extremely rough after this process due to non-uniform alloy regrowth regions. However, this does not have any significant effect on the subsequent contact metallizations.

F. AR Coating

The development of the tantalum pentoxide (Ta_2O_5) antireflecting coating began by establishing a process for the vacuum deposition of this material, followed by a study of all controllable parameters to optimize the process. Specific goals at the outset of this program were 1) to achieve an index of refraction of 2.15 (optimized for Teflon); 2) to minimize absorption, especially in that region of the spectrum below 4500Å; and 3) to provide a repeatable process compatible with shallow diffused cells.

Electron beam deposition was chosen as the most suitable method for obtaining optical quality Ta_2O_5. Several types of Ta_2O_5 were investigated initially; loose powder, chunks of compressed powder, and sintered tablets. The last mentioned type was found to be most suitable because it did not exhibit rapid cratering or the tendency to spatter common to the other forms.

Using this material, a baseline value was established for each of the following parameters: 1) deposition rate; 2) substrate temperature; and 3) chamber pressure. An optical monitor was employed to provide a relative indication of absorption and index of refraction.

A schematic of this system is illustrated in Figure 8. The system consists of a masked circular transparent chip plate on which 24 different regions can be selected and AR coated in a single vacuum pump down. The principle of operation consists of transmitting a constant voltage light source to the chip plate by means of a fiber optic guide and the reflection of this incident light through a second guide to a narrow bandpass (5500Å) filter and solar cell light detector. The solar cell current is then amplified and fed into a strip-chart recorder. The light initially transmitted through the light guide is chopped at a frequency identical to that of the amplifier so that stray radiation from the evaporant and background does not interfere with the reflected light signal and subsequent detector output. From this recording the deposition rate, thickness, and refractive index of the deposited film can be monitored. By simply revolving the chip plate, a complete series of films can be deposited to determine the necessary deposition parameters.

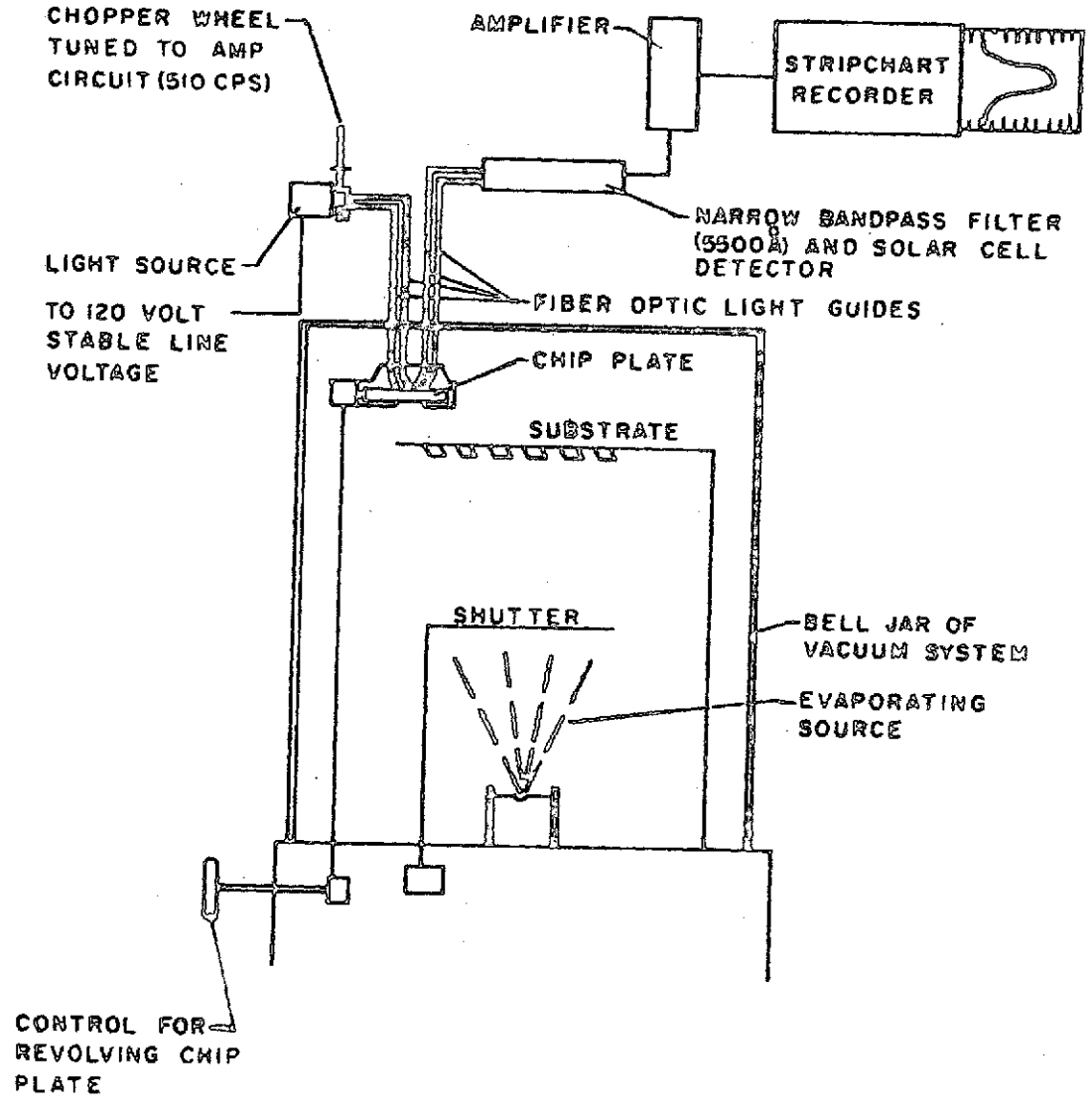

Figure 8. Optical Monitoring System

Evaporation parameters were varied over a wide range of values. It became evident that the most important factor determining the coating characteristics, absorption and index was the chamber pressure during deposition. Index of refraction increased as chamber pressure decreased. At the same time, however, the amount of absorption also increased. Increasing chamber pressure from a low initial value by backfilling with oxygen was quite effective in reducing absorption, but the index decreased accordingly.

A number of quartz witnesses were then coated and transmission traces in the region 3000 Å---12,000 Å were recorded on a spectrophotometer. The index of refraction of these coatings as calculated from the transmission traces was approximately 2.1. Also, significant absorption was evident below 4000 Å. In order to eliminate this absorption, the Ta_2O_5 coated quartz samples were baked in air at 300°C for 30 minutes. Also, additional samples were made using an oxygen bleed into the deposition chamber during the coating process. Both of these techniques were successful in reducing absorption. The oxygen bleed technique, however, tended to reduce the index of refraction of the coatings to values as low as 2.0.

Using the preliminary data obtained with quartz witnesses, a series of depositions using solar cell test samples was made. The percent appreciation in test cell output of short circuit current, current at a fixed load, open circuit voltage, and the relative spectral response at each of 13 discrete wavelengths between .4 and 1.05 μM was recorded, as well as the substrate temperature, deposition rate and chamber pressure for each run.

The process parameters of temperature, rate, and pressure were each varied over a wide range of values in order to determine their effects on the resulting coating and thus provide the information necessary to optimize that coating. Substrate temperature was varied from 100°C to 300°C in 50°C increments. Little change in coating index and transparency was observed above 150°C. However, below that value absorption was very high and the mechanical properties (hardness and adherence) of the coating were very poor. Above 250°C some evidence of contact punch through was observed for shallow diffused cells. A final value of 200°C was thus chosen as the optimum substrate temperature, and this value remained constant throughout the remainder of these experiments.

Deposition rate was varied from 1 to 10 Å/sec. Equally good results were obtained throughout this range and a convenient value of 4 Å/sec. was chosen.

Chamber pressure during deposition was initially a self-determined value dependent upon the outgassing rate of the source material and the pumping speed of the system being used. For the same E-gun power level, .75 KW for example, chamber pressure could be as high as 8×10^{-4} torr with new source material or as low as 5×10^{-5} torr with an old source, a result of the changing composition of the source material with use. The major effect of these differences in pressure from run to run was to produce changes in the index of refraction and absorption, both increasing inversely with pressure. In order to gain some control of this parameter, it became standard procedure to premelt new source material at relatively high power levels until the chamber pressure dropped to a desired value of 1.5×10^{-4} torr at deposition power.

A large number of cells were then coated using this technique. Short circuit current gains in air as high as 41 percent were recorded. However, it was evident from spectral response data that the coatings were slightly absorbing below 5500 A, even after a post deposition heat treatment. For this reason, the chamber pressure during deposition was increased to 5×10^{-4} by bleeding back oxygen. A substantial reduction of absorption in coatings deposited at this higher pressure was thus obtained. The index of refraction was reduced slightly to a value of 2.05 - 2.10. Short circuit current appreciation of cells coated using this technique was in general 1 to 2 percent higher in air and approximately equal when covered with glass coverslides, as compared to cells coated at lower pressure without oxygen. However, the oxygen bleedback technique made chamber pressure a controlled parameter, no longer dependent on the state of the source material, and for this reason became the standard procedure.

However, this procedure did not eliminate the necessity of heat treating the cells after deposition. It was found that very short periods of heating in air (30 sec.) would remove almost all absorption, and a two minute bake cycle was chosen as the standard post deposition bake time. The improvement in cell output obtained by this technique is readily apparent from the change in relative spectral response as shown in Table 4 for a typical test sample.

G. Wraparound Cells

Once the other aspects of advanced cell technology were reduced to practice, attempts were made to incorporate them into a thin (0.20 mm) 2 x 2 cm wraparound configuration. Of the four major improvements, the new Ta_2O_5 anti-reflection coating and the thin grids obviously presented no difficulty. Thus our efforts concentrated on studying the feasibility of using a back surface field and a more shallow junction in the fabrication of thin high efficiency wraparound cells.

There were two methods available to us for providing the back surface field: diffusion of boron or evaporation and subsequent diffusion of aluminum. Since the latter technique would automatically provide both N+ and P+ conductivity regions on the back surface due to the masking properties of aluminum, it was chosen for this work.

Initial experiments were performed to judge the effect of partial back field region on the cell's performance. During the aluminum evaporation, approximately eight percent of the wafer's rear surface was masked along one edge, corresponding to the area that would be lost in a typical wraparound structure. After the phosphorous diffusion, the back surface consisted of an aluminum doped P+ region with a phosphorous doped N+ region adjoining it. The cell was then contacted in the normal fashion, except that the back contact was deposited only within the P+ region. Following this, the cell was edge etched to isolate the rear N+ contact and to eliminate any shunting between the junction and the back field region. However, the back surface field still was joined to the phosphorous diffused region on the back of the cell. Eight cells were fabricated in this manner.

Wavelength (nm)	Relative Spectral Response Appreciation (%)
.400	15
.45	9
.50	5
.55	3
.60	2
.65	1
.70	1
.75	0
.80	0
.85	0
.90	0
.95	0
1.05	0

Effect of Post Heating

on Spectral Response

Table 4

Electrical measurements at 25°C under AMO conditions were performed. These cells, although not AR coated, had open circuit voltages in excess of 585 mV and short circuit currents approximately 10 percent greater than non-field cells. The fill factor was poor due either to the fact that the heavily doped regions on the back of the cell were still in contact with each other, due to incomplete edge etching, or to the reduced rear contact area. However, the experiment was a success in that it demonstrated the feasibility of wraparound configurations with back surface fields.

A number of wraparound configurations were evaluated and a front spine wraparound with a single rear pad was chosen (see Figure 9). This design minimized back contact loss and also used only a very small portion of the cell edge for the actual wraparound contact. While this tooling was being procured, some wraparounds were made using tooling from a previous NASA/Lewis contract. However, instead of two separate evaporations, the contacts were deposited in a single pumpdown using rotisserie tooling which rotated the parts during the contact deposition. A shallow diffusion, yielding a sheet resistance of ~120 ohms/□, was used for these cells. Short circuit currents approaching 160 mA and open circuit voltages exceeding 580 mV were achieved, but the curve shape was relatively poor, probably due to shunting from the full wraparound edge contact. Another possibility is that the actual wraparound portion of the contact adheres poorly due to angle of incidence effects.

Cells were fabricated using the spine configuration; and even though the wraparound pad only used ~3 percent additional back contact area, the fill factors were still poor - FF ~0.70 was representative. We feel that this poor fill factor can be partially explained by the fact that the cells are very thin and thus more susceptible to edge chipping, which was the main cause of poor fill factors in the past. We found it necessary to target the diffusion to yield a value of ρs of ~60 ohms/□ for wraparound cells. Further discussion of wraparound problems and possible explanations will be found in a subsequent section of this report.

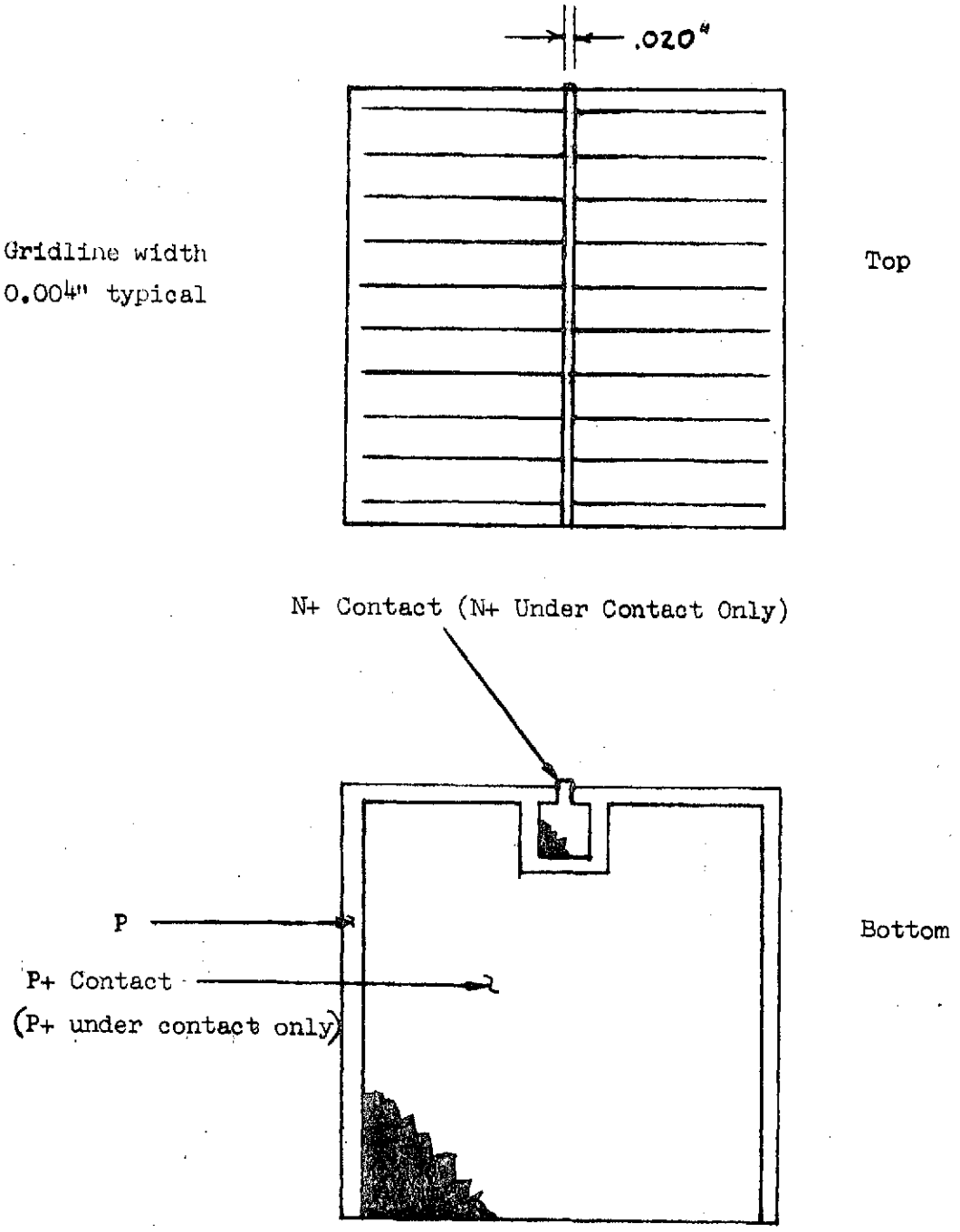

Figure 9. Wraparound Spine Configuration

IV. CELL FABRICATION

Three types of advanced solar cells (all 2 x 2 cm) were chosen for the cell fabrication phase of this contract: 1) an Aℓ BSF cell; 2) a boron BSF cell; and 3) an Aℓ wraparound BSF cell. All types were made from 0.20 mm thick 10 ohm-cm material. The conventional BSF cells had sheet resistance values of ~100-150 ohms/□ , while the wraparound cells had ρ_s values of ~60 ohms/□ .

A. Aluminum Back Surface Field Cell

Process flow charts showing the basic fabrication steps for each type of cell are given in Tables 5 through 7. The material for all cell types was prepared in the same manner as is typically done in standard production. In the case of the Aℓ BSF cells, the acceptor doping source was deposited on one side of the cell using resistive heating techniques. The conventional cell was completely coated with aluminum, but the wraparound was masked in such a manner as to form the final back contact configuration after diffusion (see Figure 10). It is very important that the amount of aluminum be at least five microns thick in order to obtain a good field cell. This is strictly an empirical observation, and we do not understand the relationship between cell output and aluminum source thickness.

The wafers were then diffused using phosphine in a carrier gas of nitrogen and oxygen to simultaneously form the shallow junction and the back surface field. Diffusion times between twenty and thirty minutes at a temperature of 825°C were sufficient to form a shallow junction and a back surface field.

After cooling, the cells were put through a special cleaning process to remove the aluminum residue from the rear surface. This process uses hydrochloric acid to first dissolve most of the aluminum, followed by ultrasonic cleaning to remove any traces of residue that might remain.

Since the aluminum-silver contact system had not been reduced to practice, passivated silver-titanium contacts were deposited. To avoid front junction degradation, the back contact was evaporated first and then sintered to break down any electrical barriers that might exist. In many cases, it was possible to completely eliminate sintering due to the high surface concentration of aluminum acceptors; but for this phase of the work, all cells were sintered. The cells were then given a thirty second soak in 10 percent HF to remove the oxide layer from the front surface. Front contacts were deposited through bimetallic masks in order to form the eighteen grid collector pattern.

Tantalum pentoxide (Ta_2O_5) was evaporated onto the cells to reduce reflection losses. This was done using electron beam evaporation with the cells heated to a temperature of between 150 and 200°C. Deposition rates of the order of 4 Å/sec. were typically used. Following cool-down and venting, the cells were baked in air at 300°C for two minutes in order to clear up any absorption in the Ta_2O_5 coating. After tape testing and mechanical inspection, the cells were electrically tested and graded for shipment.

Aℓ BSF CELL FABRICATION FLOW CHART

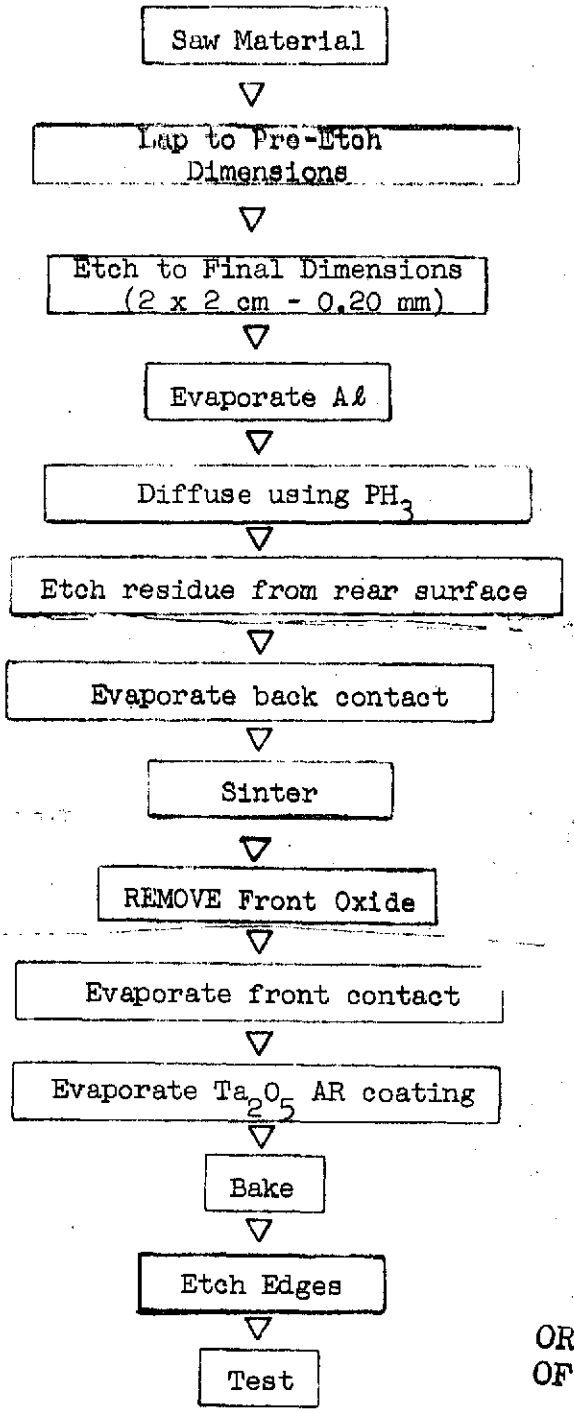

Table 5

BORON BSF CELL FABRICATION FLOW CHART

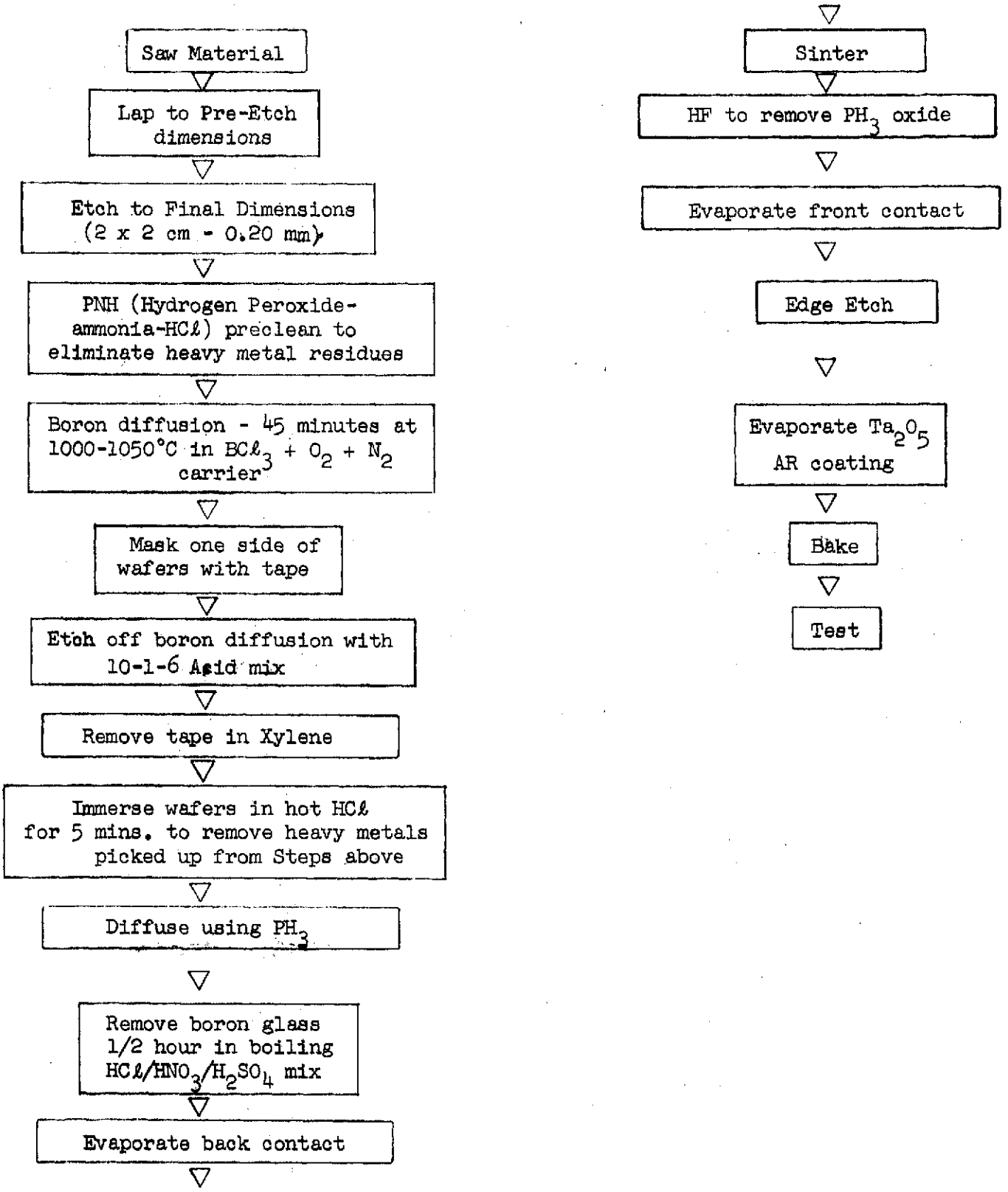

Table 6

WRAPAROUND ALUMINUM BSF CELL FABRICATION FLOW CHART

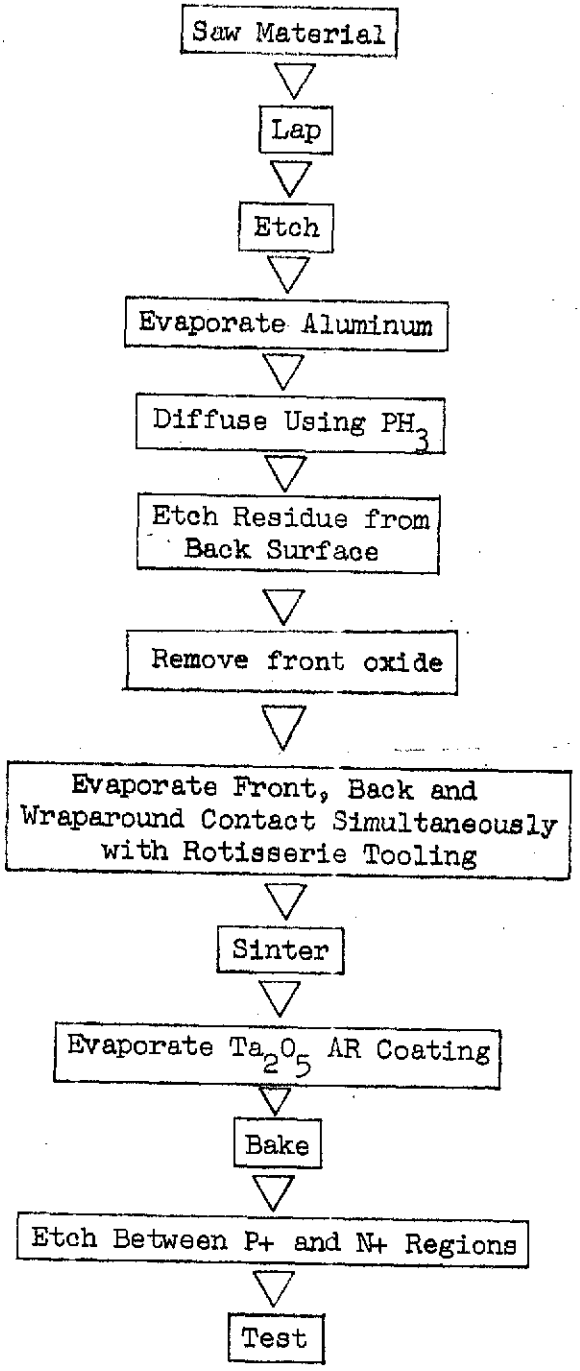

Table 7

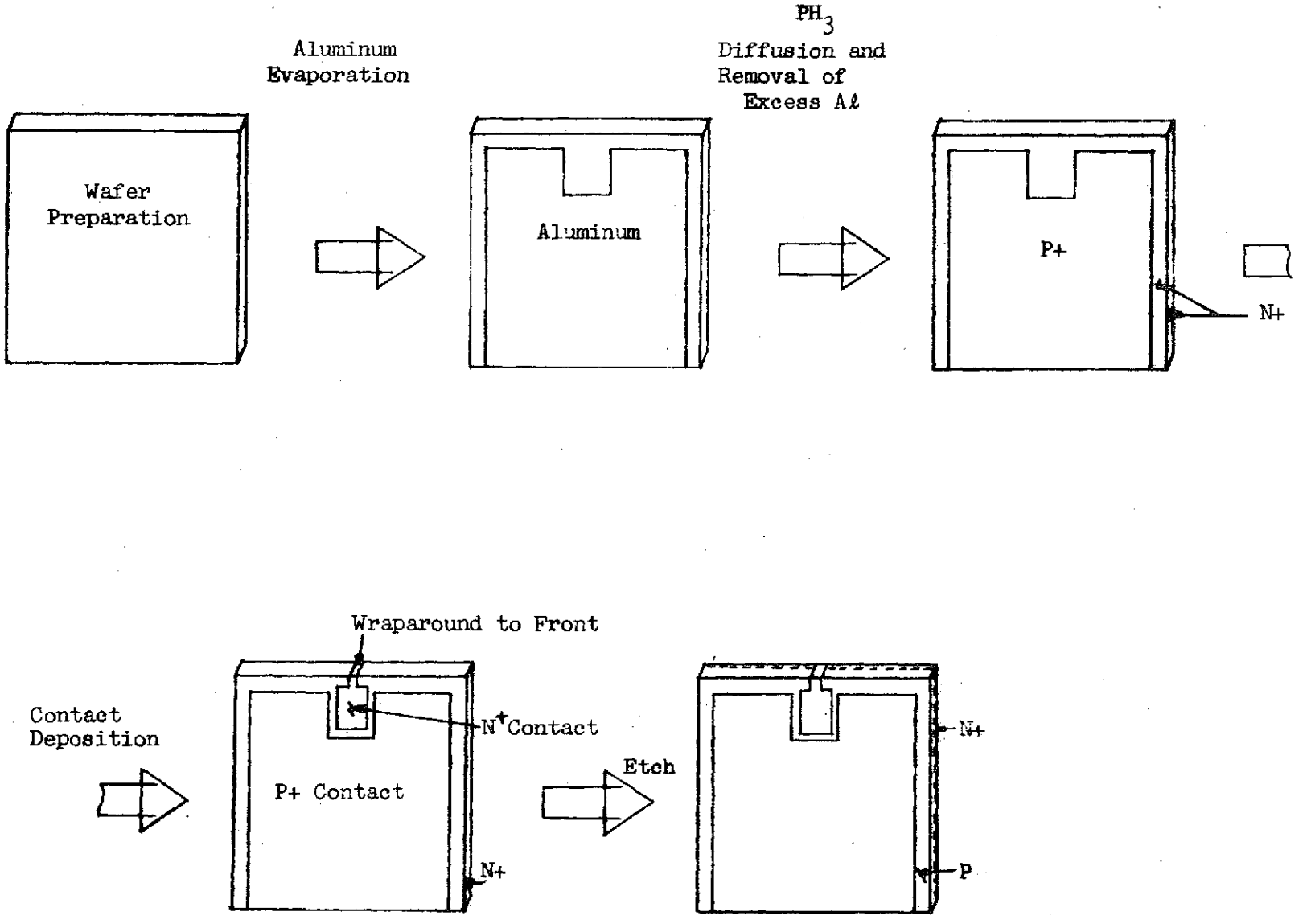

Figure 10 Wraparound Fabrication Schematic

B. Boron Back Surface Field Cell

Table 6 is a process flow chart for the boron back surface field cell. After etching the blank to its final dimensions, the silicon was given a special cleaning in a mixture of hydrogen peroxide, ammonia and hydrochloric acid in order to reduce the concentration of heavy metals which would otherwise diffuse into the material during the field formation step. The wafers were then diffused for 45 minutes at a temperature between 1000 and 1050°C using $BC\ell_3$ in a carrier gas of nitrogen and oxygen.

Upon cooling, one side of the wafer was masked with tape and then placed in a 10-1-6 (HNO_3-HF-CH_3COOH) acid solution for approximately two minutes in order to remove the boron diffused layer. The tape was removed using xylene and the wafers immersed in hot $HC\ell$ for five minutes to remove any heavy metal residue that may have been taken up from the previous etch.

The wafers were then diffused, using phosphine as the doping source, for twenty minutes at 825°C. After cooling, the wafers were boiled for thirty minutes in an acid solution of $HC\ell$,HNO_3 and H_2SO_4 in order to remove the boron glass from the rear surface. The remaining fabrication steps were identical to those used for the aluminum back surface field cells.

C. Wraparound Aluminum BSF Cells

The process flow chart for the wraparound contact cells fabricated for this contract is shown in Table 7 . A conventionally prepared wafer is aluminized using a wraparound-type back contact evaporation mask, thus establishing the $A\ell$ P+ region as being identical to the back contact area. The aluminized wafer is then diffused at 850°C for twenty-five minutes to obtain a ρ_s of $\sim$60 ohms/$\square$. Excess aluminum is removed and the part cleaned in the usual way prior to contacting. Ti-Pd-Ag contact evaporation is accomplished in one step using rotisserie tooling and special wraparound contact evaporation masks. After taping the front surface, contacted cells are dipped in 3-1-2 (HNO_3-HF-CH_3COOH) etchant for ten seconds to etch a region between the N and P contacts on the back surface, and to etch the cell edges not covered by the contact, thus creating the desired N+, P, P+ transition. Finished cells are then AR coated with Ta_2O_5 and tested.

V. CELL TESTING

The 250 advanced solar cells were tested prior to shipment to typical space flight qualification standards. This included electrical and environmental performance tests. This section describes the various tests and pertinent results. All three types of cells, aluminum BSF, boron BSF, and wraparound were tested accordingly. Prior to the environmental tests, all cells to be evaluated were mapped for initial defects. A typical map of a cell is shown in Figure 11. After each test sequence the cells were once more examined and compared to the initial maps.

Tape Test All fabricated cells were subjected to a tape peel test using Scotch Brand No. 810 tape. All front contacts were tested; however, in view of the cell thickness (.020mm), only ten percent of the back contacts were tested to minimize the possibility of excessive cell breakage. In the case that any of the tested back contacts did peel, then the test was extended to all cells in that particular lot. Cell failure occurs when any front contact bar peeling occurs, when more than one gridline peels, or when back contact peeling exceeds two percent of the contact area. All of the 250 delivered cells passed this test.

Boiling Water A quantity of cells, equal to 3 percent of the delivered cells, were suspended in boiling DI water for 30 minutes, after which they were dried and subjected to a standard tape test. No AR coating peeling was observed.

Erasure Test Three percent of the cells were erased on the front surface using a standard pink pearl eraser. After 20 rubs (20 oz. pressure) the AR coatings were examined. No Ta_2O_5 coating removal was observed.

Thermal Shock Ten percent of all cells were subjected to a 10 cycle test from + 140°C to -196°C. The rate of at least 30°C/minute was attained by immersion in liquid nitrogen for the low temperature limit, then transferring them to a hot plate for the high temperature sequence. A one-hour dwell at each temperature extreme was included as part of the test. There was no occurrence of AR coating peeling or other physical damage.

High Temperature-High Humidity A quantity of cells, equal to 10 percent of the delivered cells, was subjected to a 5 day high humidity, high temperature storage test. Test temperature was 45°C with a relative humidity of 90 percent. Subsequent tape testing showed minimal contact peeling and electrical testing results showed no appreciable electrical change (i.e., ≤ 2 percent).

Cell Output All cells passing the initial tape peel test were electrically tested with a Spectrosun® X-25 xenon solar simulator at AM0, 28 ± 1°C conditions. Complete I-V characteristics were obtained along with I_{sc}, V_{oc}, and P_{max} values. The best cells were selected for shipment to NASA Lewis and fill factors were calculated for these cells. Typical V-I characteristics for cells sent to NASA Lewis are shown in Figures 12 through 16. These include aluminum and boron BSF cells and wraparound contact

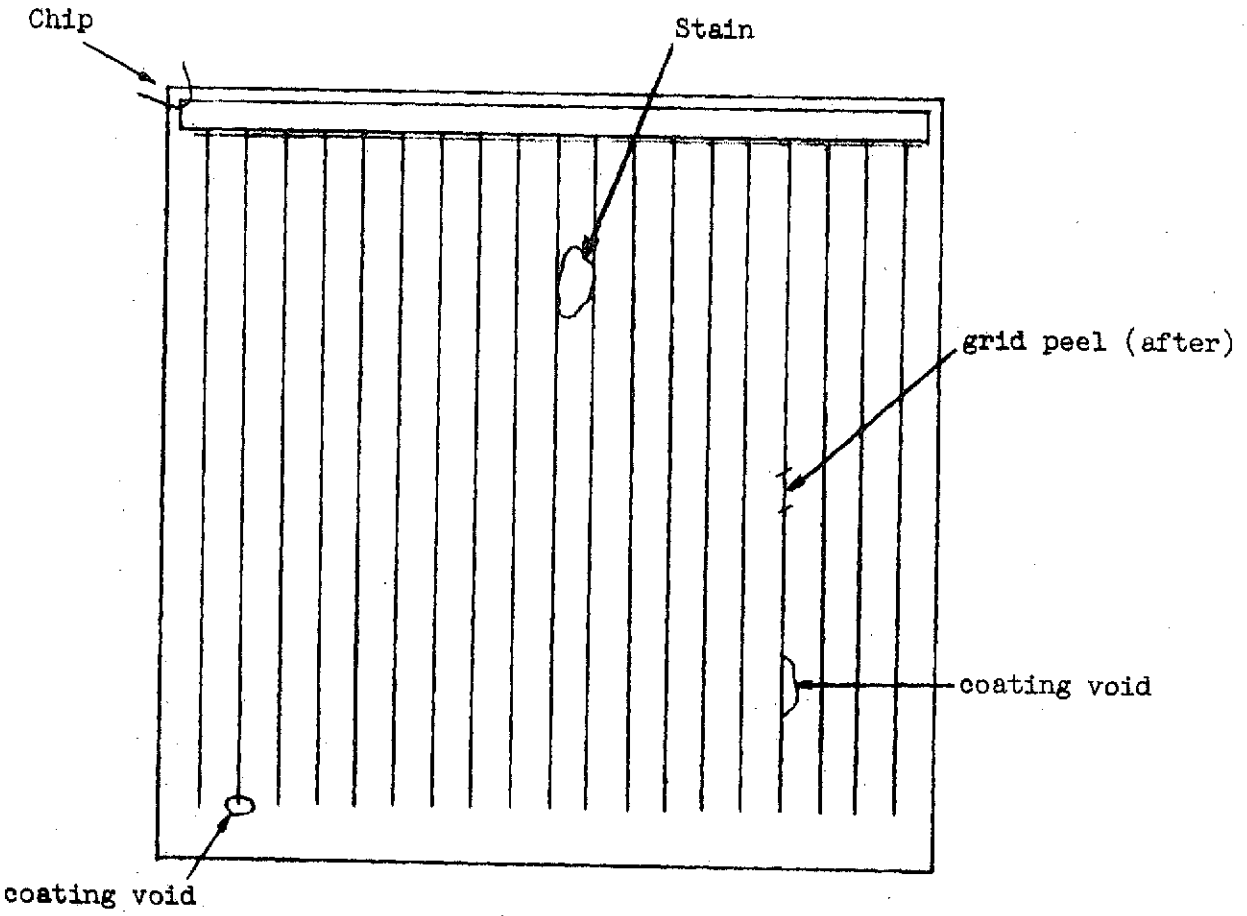

Figure 11. Cell Map Before and After Humidity Test

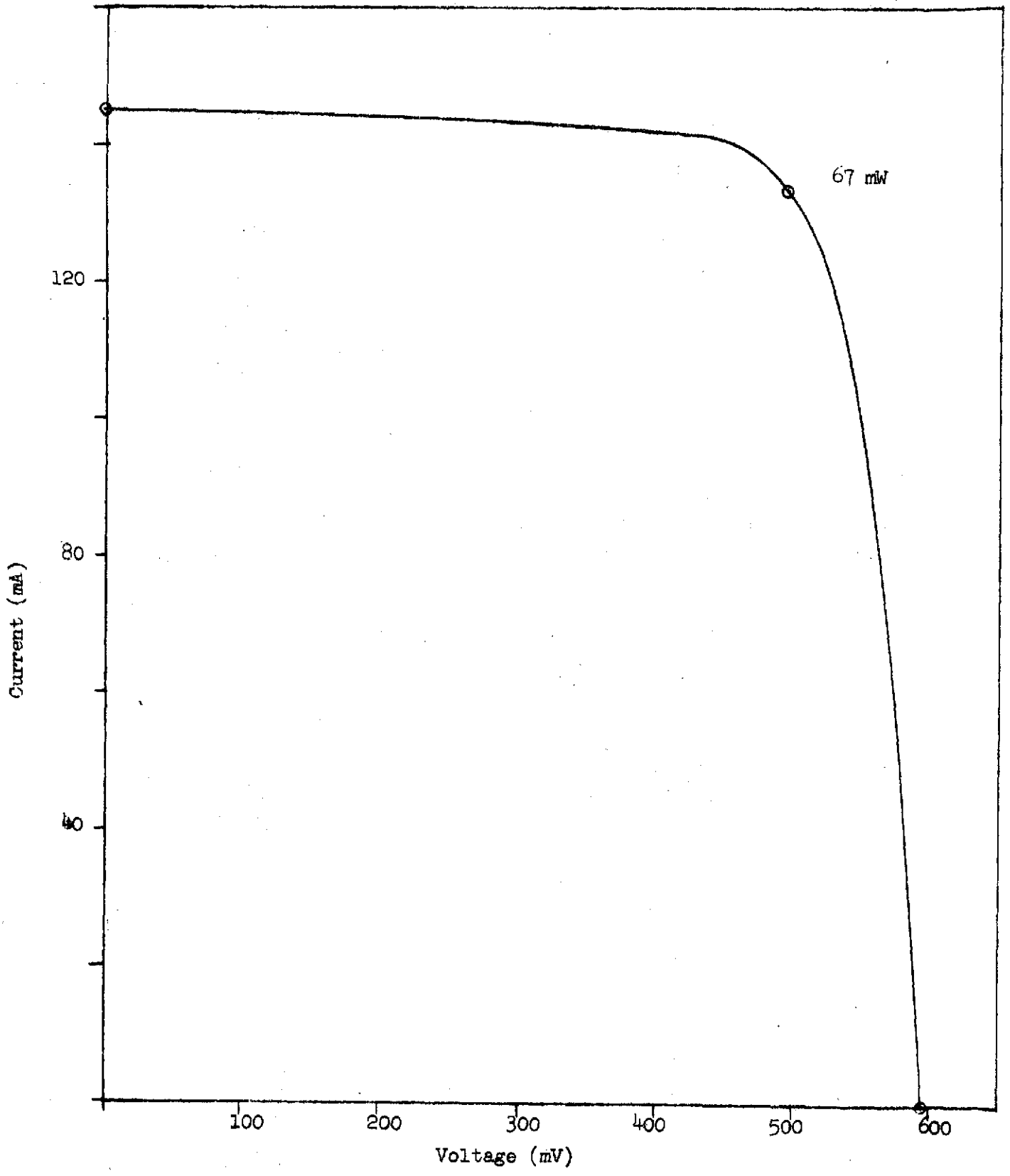

Figure 12. Typical Final Boron BSF Cell

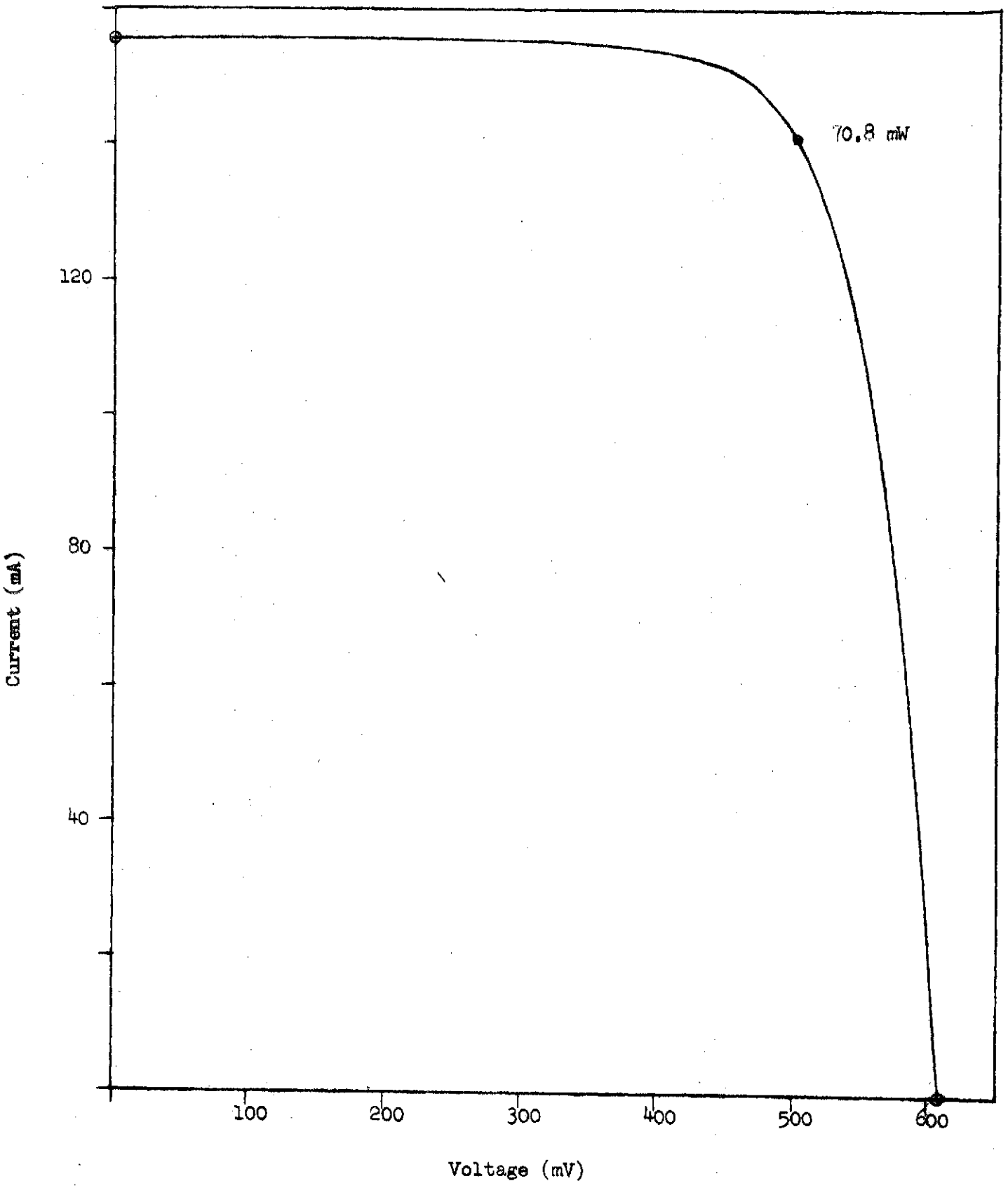

Figure 13. Typical Final Boron BSF Cell

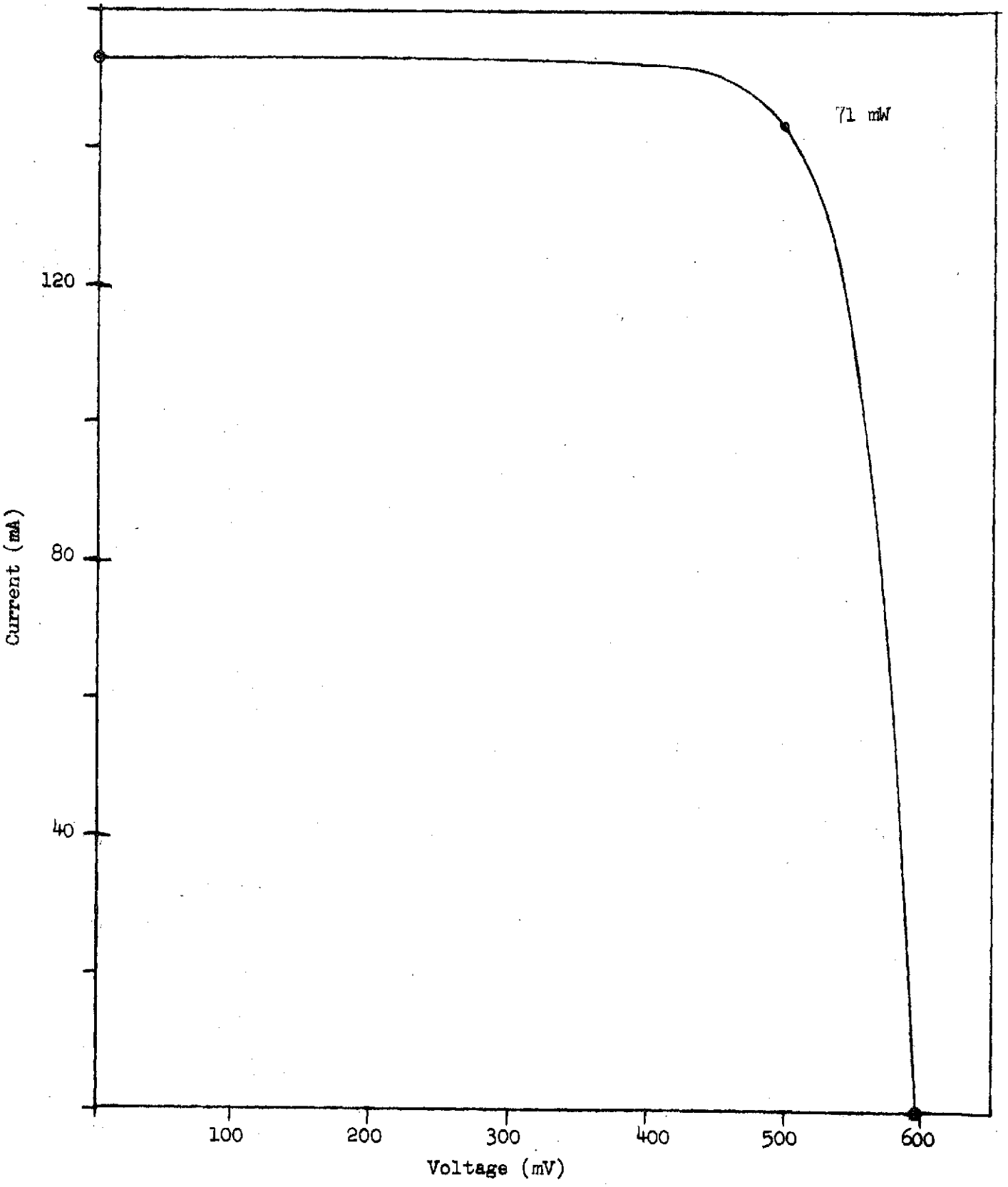

Figure 14. Typical Final Aluminum BSF Cell

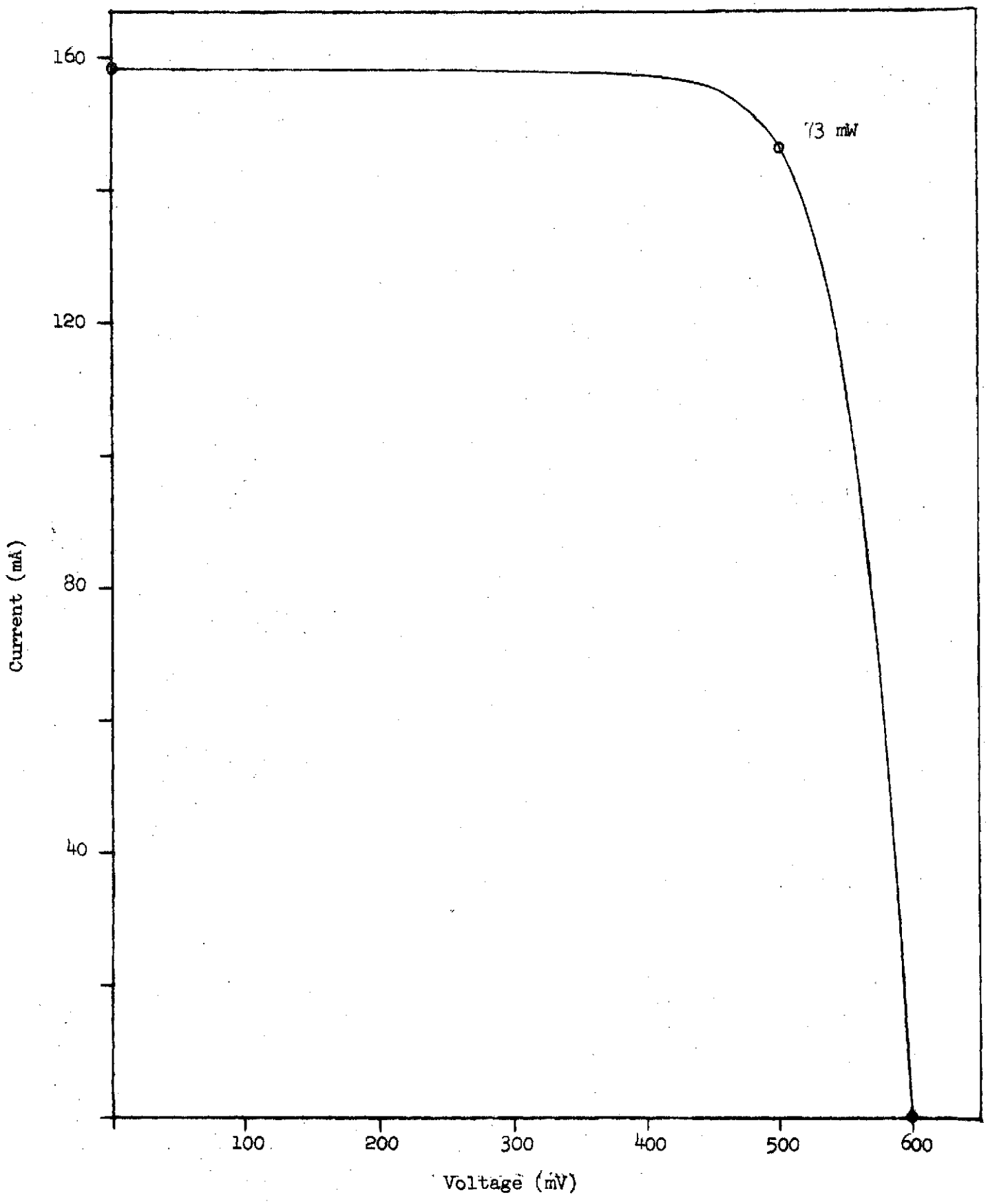

Figure I5 Typical Final Aluminum BSF Cell

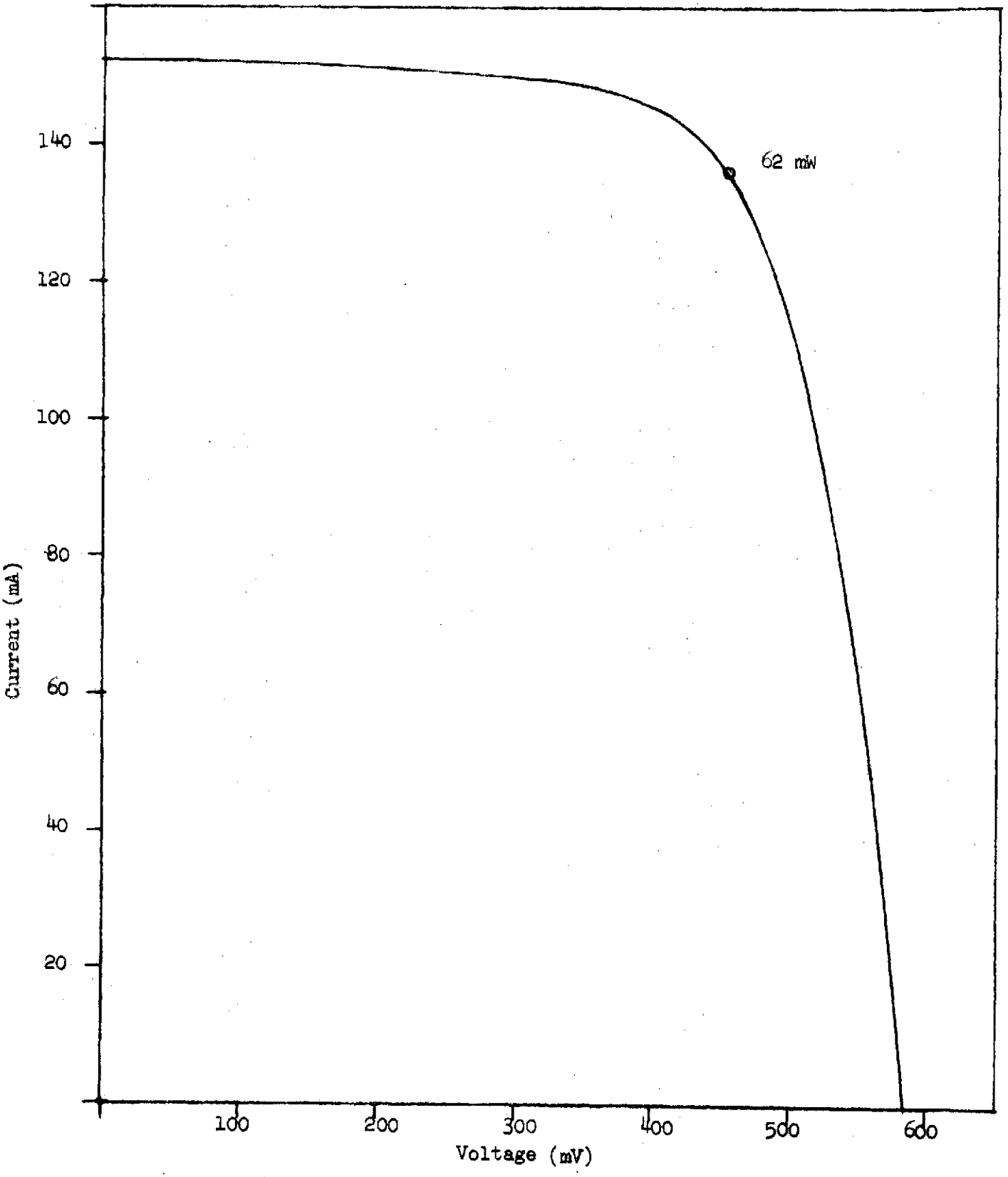

Figure 16. Typical Final Wraparound Aluminum BSF Cell

cells. In addition pertinent performance data is supplied in Figures 17 through 20, for the distribution of cell I_{sc}, V_{oc}, P_{max}, and fill factor respectively. In addition to the above, Figures 21 and 22 show typical spectral response curves for aluminum and boron BSF cells.

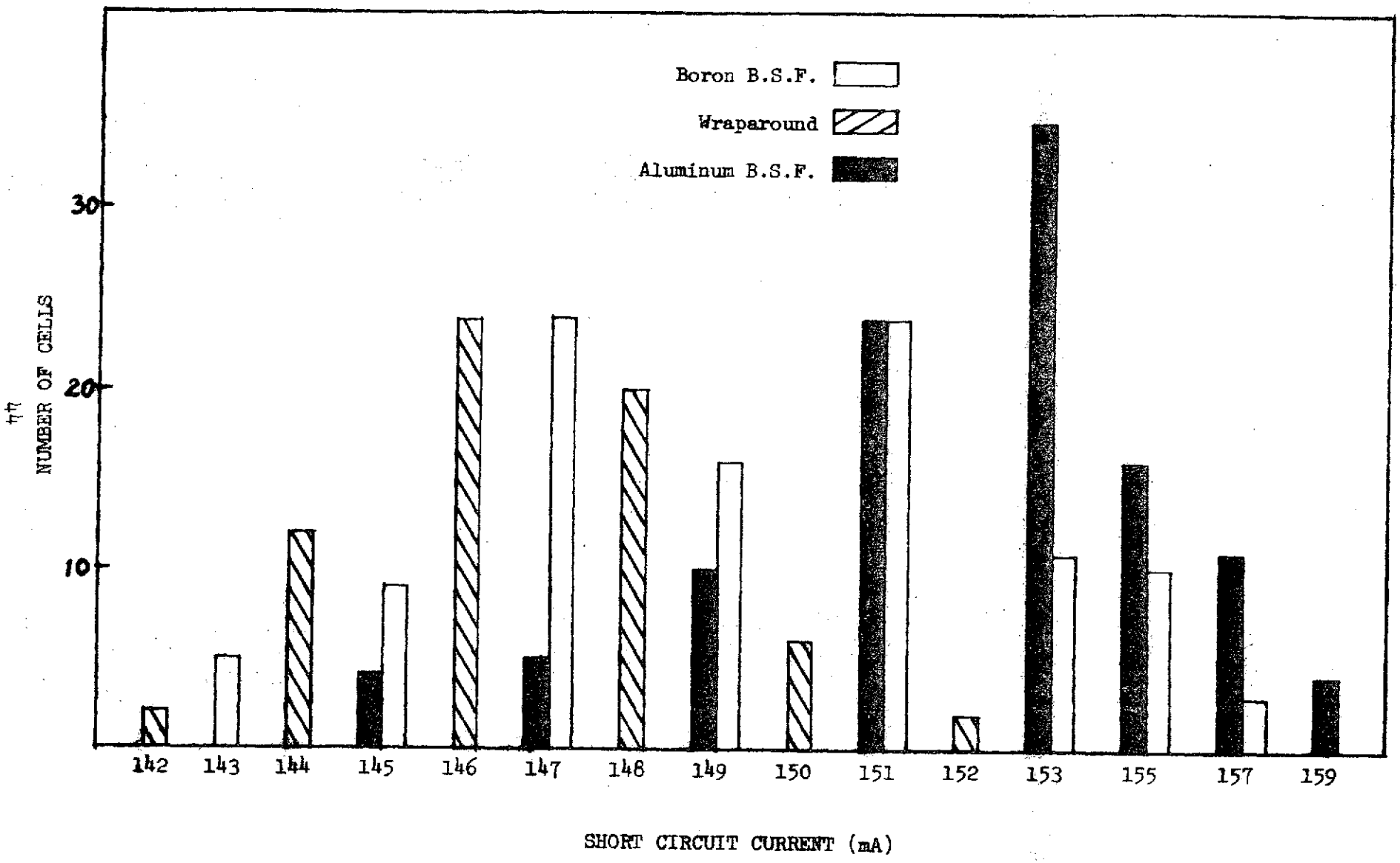

Figure 17 Cell Short Circuit Current Distribution

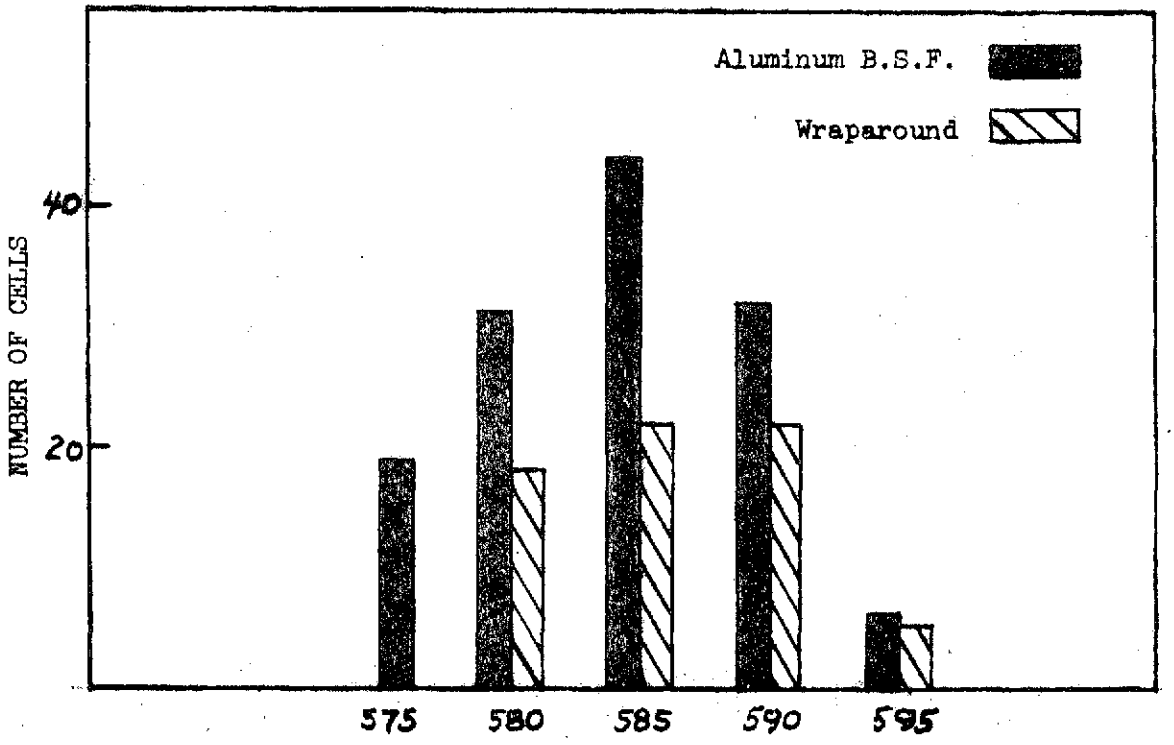

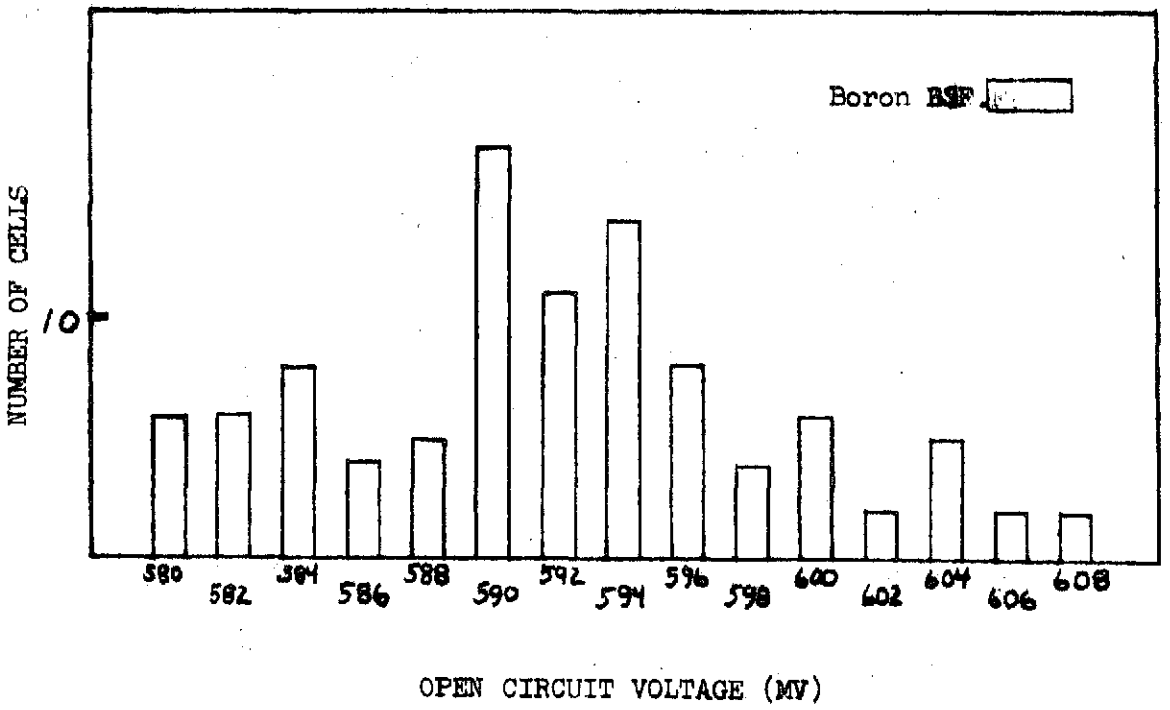

Figure 18 Open Circuit Voltage Distribution

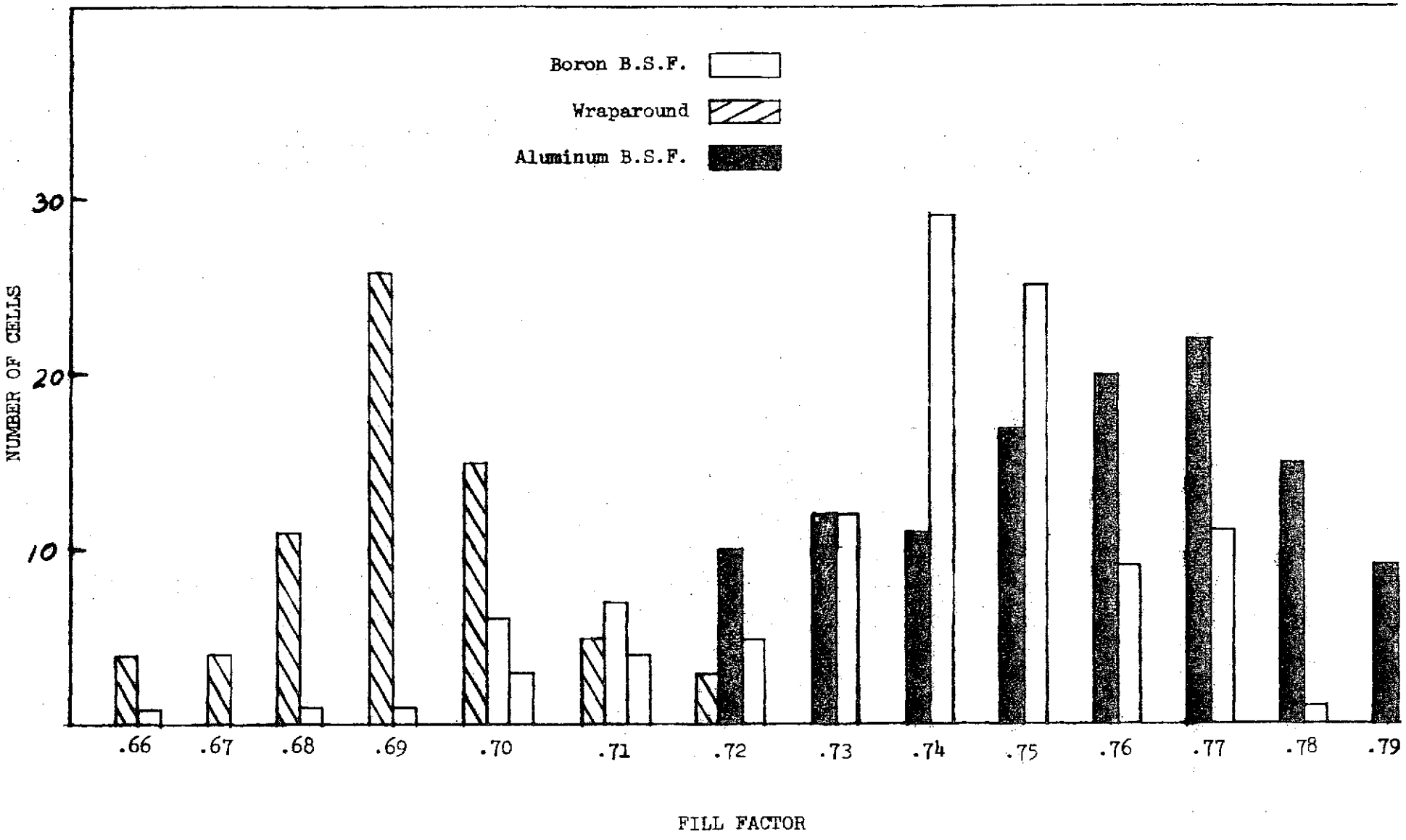

Figure 19 Fill Factor Distribution

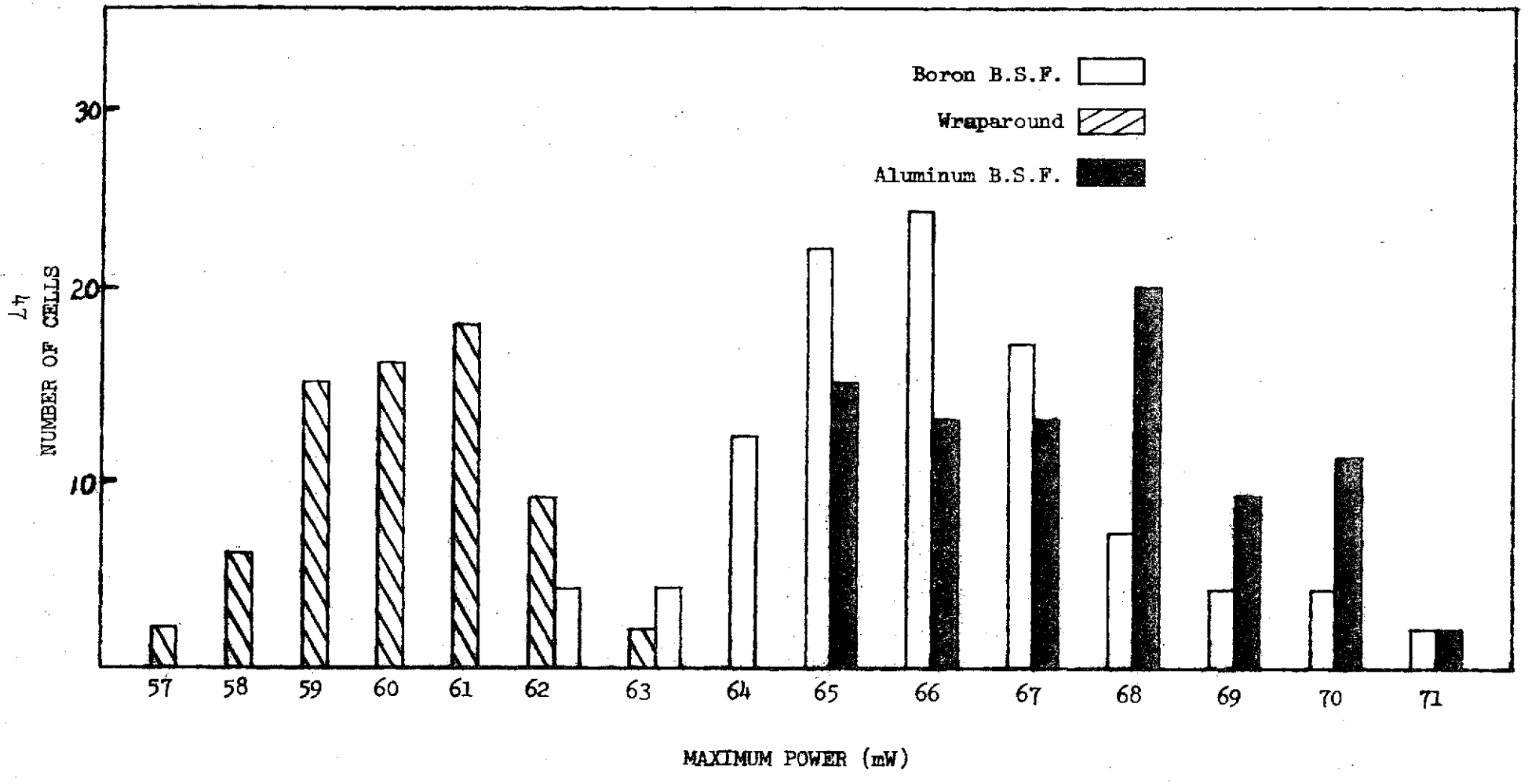

Figure 20 **Maximum** Power Distribution

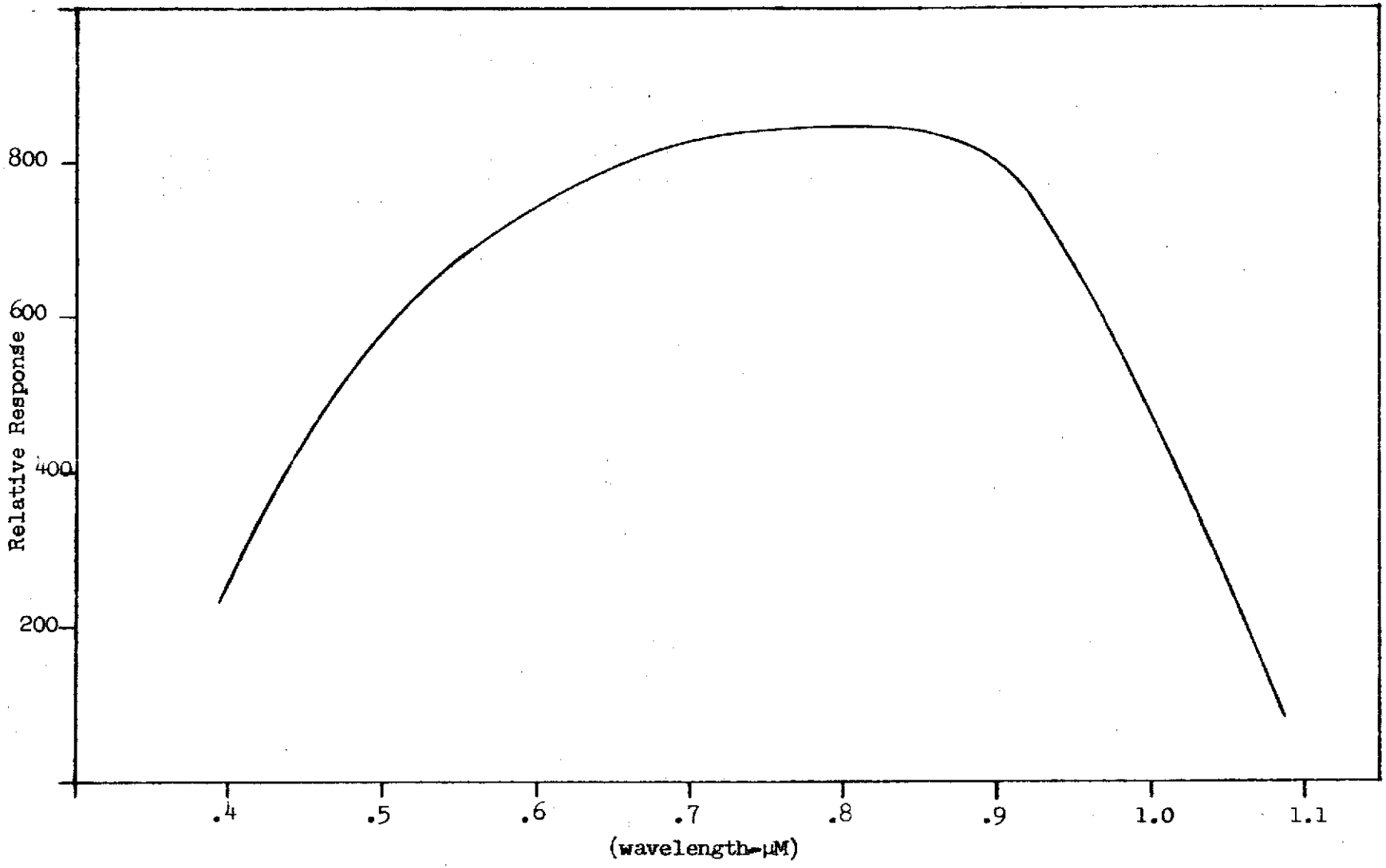

Figure 21. Typical Aluminum BSF Cell Spectral Response

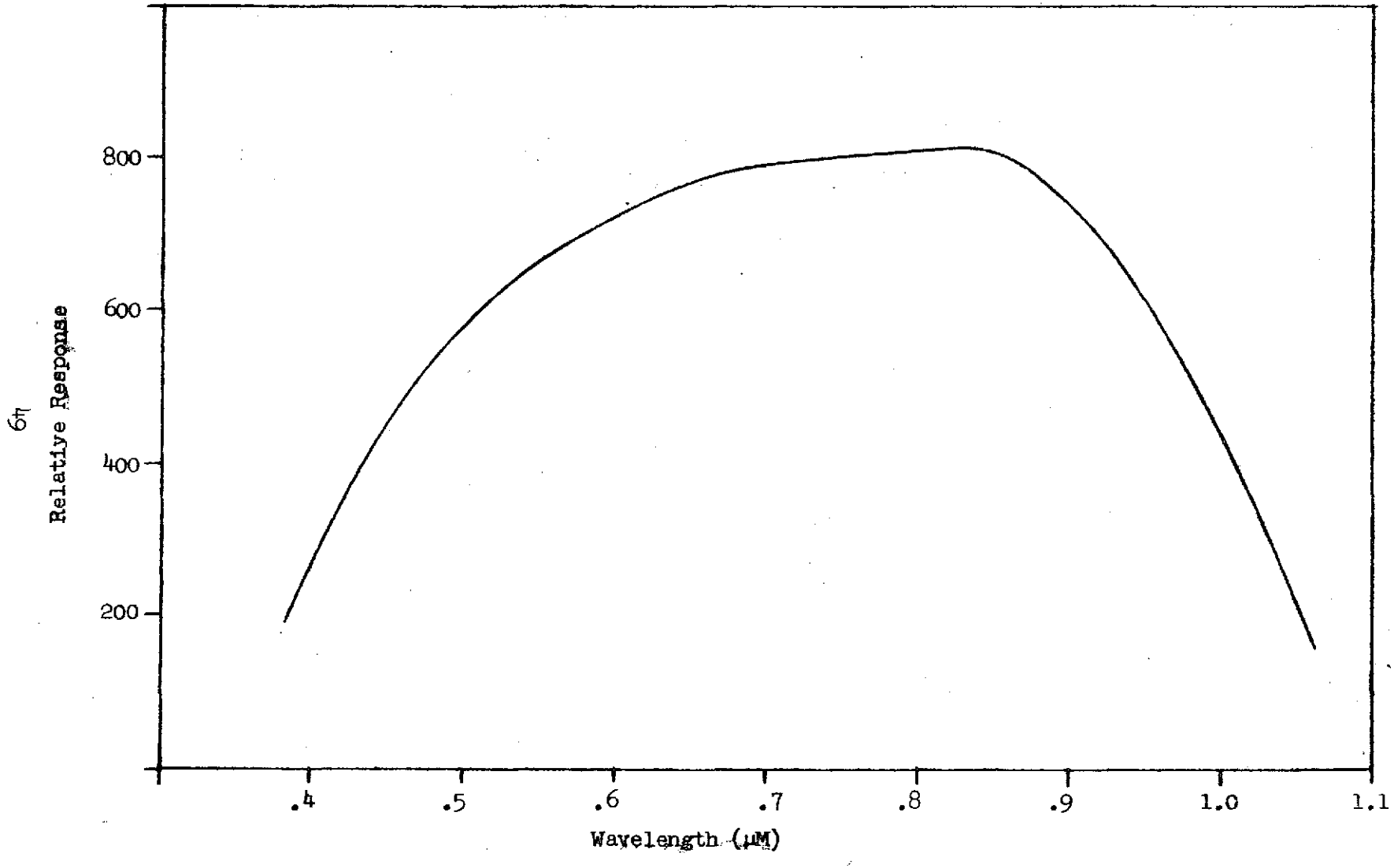

Figure 22. Typical Boron BSF Cell Spectral Response

VI. DISCUSSION

A review of the data generated from the 250 cell pilot run shows that significant progress has been made toward the goals of this contract. A number of compromises were made and this was to be expected in view of the fact that the ultimate objective was to develop processes that could be used for high volume production.

The shallow diffusion work did achieve the goal of this contract which was a gain of approximately 2.5 mA/cm^2 over conventional diffusions. It was also found that sheet resistance values in excess of 150-175 ohms/$\square$ did not yield any additional short wavelength response and consequently no further improvement in short circuit current. The technique for obtaining improved short wavelength response was relatively simple, merely requiring adjustments in time and temperature without any change in the method or dopant used for junction formation.

Calculations based on known junction depths for a given ρs indicate that the advanced cells have junction depths of between 0.12 and 0.15 μM This depth still allows the cell to be interconnected in conventional fashion using either solder or welding techniques. The importance of this fact should not be over looked since the final function of most solar cells is to be assembled into circuits.

Naturally the shallow junction automatically required other advances to be made in cell fabrication. The two most important were the contact configuration and the antireflection coating. Addressing the former subject we concluded, on the basis of cost and yield rather than on technical grounds, that a compromise had to be made between the ideal situation and what could be accomplished in a manufacturing environment. Calculations showed that ten lines per centimeter, each line approximately 2×10^{-3} cm in width would yield optimized power. However, the only method of achieving this geometry required photoresist techniques. It will be admitted that finer geometries than this are routinely done in the microelectronics industry, but the value per cm^2 of silicon of their yielded devices is many times that of a solar cell. Therefore on a cost basis this type of process could not be justified.

Using this guideline we evaluated bimetallic masking for contact deposition. The bimetallic mask can be constructed to yield line widths down to 3×10^{-3}cm. It allows cells to be processed in normal fashion with respect to contacting since the standard cell is contacted using less sophisticated masks. An analysis based on a realistic line width of 5×10^{-3}cm showed that series resistance could be reduced below the levels attained with conventional junction depths without sacrificing active area from that obtained in the conventional device. A savings in active area was achieved by reducing the collector bar from the typical 1.0mm width to 0.5mm. This change was also made on pragmatic grounds since some panel manufacturers have now refined their cell assembling equipment to the point that a more narrow collector bar can be accommodated.

The work with bimetallic masks indicated certain areas where additional effort will be needed before these masks can be pronounced as suitable for large scale production. The masks require peripheral support frames which adds more complexity to assembling and maintaining them. The nickel metallization which defines the line geometry is susceptible to nicks and scratches from handling. A reliable cleaning process that does not damage the mask has yet to be finalized. At present the bimetallic masks are initially more expensive and possess a useful lifetime approximately equal to half that of a conventional stainless steel mask. The cost impact is not extreme since tooling represents only a small fraction of the final cell cost, but it should be pointed out that there is additional cost for this step in processing advanced silicon solar cells.

Turning to the antireflection coating we once more made a judgement that compromised the ultimate objective of this phase of the contract. It is well known from theoretical considerations that a multiple layer coating system will be superior to a single layer material in reducing reflection from the solar cell. However, the properties required of the multiple layer system restrict the choices of materials that can be used. Not only must the components be relatively free from absorption, they must also be durable and stable under the operating conditions encountered in the space environment. Finally, there is the concern for the reliability that can be achieved with a multiple layer process in a manufacturing situation. From these considerations we felt that a single layer film possessing better short wavelength transmission and a higher index of refraction than the conventional silicon monoxide coating would be a significant advancement.

One of the goals for this phase was to develop a coating system that would be a proper match to Teflon FEP which is under serious consideration as a replacement for the present fused quartz protection systems. Our experience indicated two potential single layer candidates, titanium oxide (TiO_x) and tantalum pentoxide (Ta_2O_5). From the standpoint of refractive index, both materials were acceptable. Examination of their transmission showed that below 4000 Å Ta_2O_5 was superior. Based on this fact alone we chose to develop the tantalum pentoxide coating. It should be pointed out here that in the event fused quartz is retained as a protective system and it is deemed necessary to reject certain portions of the ultraviolet spectrum in order to protect against adhesive darkening there would be no reason for not using TiO_x. However, based on the Teflon FEP system it was proper to investigate tantalum pentoxide. Our results with this material have yielded a coating with an index between 2.10 and 2.20 which is effectively transparent beyond the useful solar spectrum. An index of 2.10 is optimum for the FEP system.

There is one other aspect of advanced cell technology that also requires changing with the advent of the shallow junction, and that is the contact system. We were initially faced with the problem of compatibility between the silver-titanium system and shallow junctions. It is known that impurities related to the titanium can effectively degrade the cell during a post contact high temperature process. To avoid this problem it was suggested that an alternate to titanium be found which could be deposited in sufficiently pure form to avoid this behavior. Aluminum, although an acceptor, could be substituted provided the amount of aluminum could be

precisely controlled in order to not punch through the junction and form a direct short. In principle elevated heat treatments would result in an alloy type bond between the silicon-aluminum and the aluminum-silver. Our work did show some partial justification for this theory, but we could not make the process work in the reliable fashion demanded by high volume production.

The results of the back surface field investigations were encouraging. Initially we were required to examine boron diffusion as an alternate approach to previous work done with aluminum. While this process was being developed, improvements were made to the original aluminum method which made it a viable production process. This allowed us to make a judgement concerning the applicability of the boron process for production. The boron field cell needs at least five critical processes; 1) a special preclean to remove heavy metals, 2) a high temperature diffusion, 3) a masking and etching step to remove the boron from one side, 4) a phosphorous diffusion and 5) a boron glass removal step. The aluminum process requires three processes; 1) evaporation of aluminum, 2) a phosphorous diffusion and 3) an aluminum residue removal step. In addition to the fact that there are fewer processes, the aluminum field cell can be diffused at significantly lower temperatures thus preserving minority carrier lifetime.

At present both processes yield high performance cells, the boron cells having slightly better voltage and the aluminum cells having slightly better currents. Comparing the two with respect to the number of critical operations required leads us to conclude that presently the aluminum process is superior for high volume production.

The one aspect of this contract that presented the most difficulty was attempting to incorporate the above mentioned advancements into a wraparound cell. The field was successfully implemented using aluminum, but truly shallow junctions could not be made without severe degradation in curve shape. There are a number of potential causes for the lower fill factors observed for wraparound cells. Edge defects, such as nicks or chips, caused after the diffusion would expose bulk regions and act as shunt paths if covered by the wraparound contact. This possibility is increased as the cells become thinner and therefore more susceptible to handling damage. The wraparound contact may not be adherent which would increase series resistance. The separation between P+ and N+ regions might not be complete, especially on the cell edge opposite the wraparound (See Figure 9). The loss of back contact area will contribute some finite increase in series resistance due to the increased path length between portions of the positive and negative contacts. The technique of using the same mask to form the field region and deposit the contact may be at fault. A slight misalignment of the part could cause contact bridging between the N+ and P+ regions.

The distribution of fill factors indicates that there is a more basic problem involved than edge chips. On a statistical basis there should be finite number of wraparound cells with at least the same fill factors as the conventional cells, if random edge defects were chiefly responsible for the low fill factors.

There is an additional piece of evidence indicating a more fundamental problem. We have used this type of wraparound configuration to produce 2 x 4 cm cells, 1-3 ohm cm bulk resistivity, with a two pad pattern on the rear surface. Over two hundred cells ranging from .020 to .035 cm, both with and without back surface fields have been manufactured. The contacts, both front and rear, were successfully tested with #600 Scotch Brand tape, although no attempt was made to verify the adherence of the edge contact. In the case of aluminum back field cells 0.20 cm thick, the average fill factor was 0.76. The only differences between these cells and those made for this program were the bulk resistivity, and the fact that the field diffusion was kept away from all edges of the cell. However if the separation etch eliminates the P+ region on the back surface, it should also remove this region from the cell edge.

Previous work done here[8] and in other laboratories[9] has pointed out that the generated carriers in the region sandwiched between the front and rear N+ region must flow through a narrow channel in order to reach the positive contact. The geometry is such that a rather large resistance is encountered in this portion of the cell which, when added to the contribution from the "normal" portion leads to a reduction in curve shape. Naturally this channel resistance would be much lower for two ohm cm material and our data would suggest that it has minimal effect in the case of two ohm-cm silicon cells.

The three groups of cells that were built and delivered to NASA/LRC represent the present state-of-the-art with respect to cells that have the potential for large quantity production. Comparing the median of the distribution for each type against the original contract goals will give us one standard for judgement. Comparing these cells against present conventional 0.20mm cells will give us still another view.

The goal for this contract was to produce cells with short circuit currents of 160 mA, open circuit voltages of 600 mV, and a fill factor of 0.76, which would therefore yield 73 mW for a 2 x 2 cm cell when measured under AMO conditions at 28°C.

The aluminum BSF cells averaged 152 mA with approximately twenty percent of the population having I_{sc} greater than 155 mA. Since the antireflection coating we used was not optimized for air, the currents are lower. Assuming a two percent appreciation would yield an average closer to 155 mA with about ten percent achieving 160 mA. The boron BSF cells averaged about two mA lower with the best currents being 157 mA. The wraparound cells, because of the deeper diffusion only averaged 148 mA, with the best cells at $\sim$ 152 mA.

There are a few areas where some slight adjustments might have yielded another two or three percent improvement in current. A slight reduction in gridline width from the actual printed dimension of 7×10^{-3} cm down to 5×10^{-3} cm would gain over two percent. There may be another one percent available from diffusion. Furthermore, the actual appreciation in current when the cell is covered with Teflon FEP could be closer to three percent than the more conservative estimate of two percent for conventional coverslides. Factoring these values into what was obtained indicates that the nonwraparound advanced cell could be fabricated in volume with a short circuit of over 160 mA when covered.

The boron BSF cells had an average open circuit voltage of 592 mV with seventeen percent exceeding 600 mV. The aluminum BSF averaged 586 with a maximum cell voltage of 598 mV. The wraparound cells were equivalent to the regular aluminum field cells. Once again we were very close to achieving the ultimate contract goal and since V_{oc} values of 580 mV could be routinely achieved we must consider this aspect of cell performance to have been successfully concluded.

With respect to fill factor we once more came very close to the ultimate contract goal except for the wraparound cells. Fifty percent of the aluminum cells and twenty percent of the boron cells met or exceeded the contract goal of 0.76 fill factor. With additional experience in cell processing fill factors exceeding 0.76 should be routinely achieved in production using the present contact configuration.

The efficiencies we achieved on this contract ranged from 11.5 up to 13.1 percent with the boron cells having an average efficiency of 12.2 percent and the aluminum cells averaging 12.4 percent. The wraparounds were lower due to the problem of curve shape, but the 11.1 percent average efficiency still represents a significant achievement when compared to present-day production cells of the same thickness.

As a result of the pilot run we conclude that 10 ohm cm 2 x 2 cm silicon cells, 0.20mm thick may be mass produced with reasonable yields to achieve an average efficiency of greater than 12.0 percent when covered. This represents a twenty percent improvement over present-day cells with this geometry. It can be expected that certain refinements in processing will lead to a further improvement in cell efficiency within the coming year.

VII RECOMMENDATIONS

This contract has conclusively demonstrated that advanced processing techniques can be put into a production environment to produce high efficiency cells. At present our production line is using many of the same types of processes examined on this contract to produce space quality high efficiency cells for use on a number of programs.

The fact that advanced cells have gone from the laboratory to production in a period of only a year indicates that there has been a profound revision in the attitude of solar cell customers. It appears that improvements in cell efficiency are making many proposed missions more feasible. Since new ideas are now apparently receiving more consideration from what has been basically a conservative market, it is imperative that the initial advances in solar cell technology be continued.

It is doubtful that significant improvements over what has now been accomplished in the area of improved short wavelength response can be made. However, the present shallow junction cell has forced us to go to process sequence (sintered back-unsintered front) for contacting that is not cost effective. As stated in previous sections of this report, we feel that the aluminum-silver system shows promise and we would recommend that work in this area continue.

The techniques for reliably producing back surface fields have been fairly well reduced to practice, but in the case of boron doping the process is too complex for utilization in production. We would suggest further work using the Emulsitone spin-on sources as an alternative to the boron trichloride gas system. The aluminum BSF cell has one significant drawback, which is the necessity of depositing very thick (> 5 μM) layers of aluminum in order to develop high voltages. This can cause problems when thin (< 0.20mm) cells are processed. We would recommend some additional work oriented toward understanding the relationship between aluminum source thickness and the resulting field effect.

In view of the fact that incorporation of the back surface field increases the open circuit voltage of ten ohm cm silicon cells to that achieved by one ohm cm it would seem that even higher resistivity silicon might be investigated. Until the advent of the field cell, the more radiation resistant higher resistivity silicon could not be fabricated into reasonably efficient devices; this is no longer the case. Another aspect of field cells that should be exploited is even thinner cells. This program demonstrated the feasibility of manufacturing 0.20mm cells; further exploratory work with a goal of 0.1mm cells might prove fruitful, especially in conjunction with higher base resistivity material. The work in this area should be oriented more toward new approaches to handle very thin cells rather than a method which will yield some devices, but will not demonstrate any potential for volume production.

Perhaps the most important work remaining to be done involves wraparound solar cells. There are a number of large solar array programs in the planning stage that are seriously considering wraparound cells. The techniques for automatically assembling such cells are being developed and it appears that significant cost savings can be achieved in panel assembly if wraparound cells are available. Unfortunately the technology for mass producing wraparound cells of any type does not exist. This fact has not yet been fully appreciated by the advanced planners and unless work begins immediately many potential multikilowatt missions will either be severely compromised or will be forced to consider other competitive forms of energy conversion.

We would strongly recommend that any additional work in advanced solar cells be primarily oriented toward wraparound cells. Implementation of the silver-aluminum system would be a key step toward this objective. In addition we would recommend a re-evaluation of the present 2 x 2 cm 10 ohm cm baseline cell. Larger cells (2 x 4 cm) and lower resistivities should be investigated. The wraparound cell thickness should not be arbitrarily chosen, but should be allowed to evolve through process improvements to an optimum which will be cost effective.

References

1) J. Mandelkorn, J. H. Lamneck, Jr., "Proceedings of 9th Photovoltaic Specialists Conference," p. 66, 1972.

2) J. Lindmayer, J. Allison, "Proceedings of 9th Photovoltaic Specialists Conference." p. 83, 1972.

3) J. H. Lamneck, Jr., L. Schwartz, A. E. Spakowski, "Proceedings of 9th Photovoltaic Specialists Conference." p. 193, 1972.

4) M. Hansen, Constitution of Binary Alloys, McGraw-Hill Book Company, Inc., New York, 1958, p. 1.

5) M. Wolf, "Limitations and Possibilities for Improvement of Photovoltaic Solar Energy Converters," Proceedings of the IRE, July 1960, p. 1246.

6) P. Payne, "Development and Pilot Line Production of Lithium Doped Silicon Solar Cells," Final Report, JPL Contract No. 953171, 1972.

7 M. Newberger, et al, Silicon, EPIC AD698342, 1969, p. 47.

8) J. A. Scott-Monck, P. M. Stella, J. E. Avery, "Design and Fabrication of Wraparound Contact Solar Cells," Final Report. NASA Lewis Research Center, Contract No. NAS3-15344, 1972.

9) R. Gereth, et al, "Proceedings of 8th Photovoltaic Specialists Conference," p. 353, 1970.